Reviewed Preprint
v1 • July 9, 2025
Not revised

Reviewed Preprint
v2 • November 18, 2025
Revised by authors

Reviewed Preprint
v3 • December 23, 2025
Revised by authors

**For correspondence:**
ivana.petrovic@unibas.ch
anne.spang@unibas.ch
stephan.grzesiek@unibas.ch

† Present address: Center for Life Sciences, Paul Scherrer Institut, Villigen, Switzerland

**Competing interests:** No competing interests declared

**Funding:** See page 30

**Reviewing editor:** John Janetzko, University of Colorado Anschutz Medical Campus, United States



# A high-resolution analysis of arrestin2 interactions responsible for CCR5 endocytosis

**Ivana Petrovic, Samit Desai, Polina Isaikina†, Layara Akemi Abiko, Anne Spang, Stephan Grzesiek**
Biozentrum, University of Basel, Basel, Switzerland

## eLife Assessment

The authors investigate arrestin2-mediated CCR5 endocytosis in the context of clathrin and AP2 contributions. Using an extensive set of NMR experiments, and supported by microscopy and other biophysical assays, the authors provide **compelling** data on the roles of AP2 and clathrin in CCR5 endocytosis. This **important** work will appeal to an audience beyond those studying chemokine receptors, including those studying GPCR regulation and trafficking. The distinct role of AP2 and not clathrin will be of particular interest to those studying GPCR internalization mechanisms.

https://doi.org/10.7554/eLife.106839.3.sa4

## Abstract

Clathrin-mediated endocytosis (CME) is crucial for regulating G protein-coupled receptors (GPCRs) via phosphorylation-dependent arrestin interactions. Despite detailed structural knowledge on the arrestin interactions with phosphorylated tails of GPCRs, the interplay between receptor phosphorylation and arrestin coupling to the CME machinery is not well understood, in particular due to the weakness and dynamics of the individual molecular interactions. Here we have characterized the interactions of arrestin2, which is activated by the phosphorylated C-terminus of the human chemokine receptor 5 (CCR5), with the main protein constituents of CME, namely clathrin and AP2 by solution NMR spectroscopy, biochemical and cellular assays. The NMR analysis revealed that arrestin2 interacts weakly with clathrin through a single binding site, independent of arrestin2 activation. In contrast, the arrestin2-AP2 interaction is stronger, requires arrestin2 activation by the CCR5 phospho-tail, and depends quantitatively on its degree of phosphorylation. These *in vitro* results are corroborated by cellular assays, which show that the chemokine-induced formation of a long-lived CCR5-arrestin2 internalization complex depends strongly on the interaction of arrestin2 with AP2, but not with clathrin. Taken together, these findings provide quantitative, atom-scale insights on the first steps of CCR5 endocytosis.

## Introduction

G protein-coupled receptors (GPCRs) represent a large family of transmembrane cell surface receptors that mediate the cellular response to a wide variety of signals. Their crucial role in many human physiological processes makes them an important drug target with about a third of existing small-molecule drugs binding to GPCRs and an enormous potential for further development (Congreve et al., 2020). To ensure precise signal transduction the receptor signaling cascade events must be tightly regulated. This is achieved by coordinating receptor interactions with various intracellular proteins, including G proteins (Weis and Kobilka, 2018), GPCR kinases (GRKs) (Komolov and Benovic, 2018), and arrestins (Gurevich and Gurevich, 2019), with the latter eventually leading to receptor internalization in a process known as endocytosis. Endocytosis is a major mechanism of GPCR signal downregulation (Hanyaloglu and

Zastrow, 2008). However, some receptors rapidly recycle back to the plasma membrane (Hanyaloglu and Zastrow, 2008), which may also serve to scavenge external ligands and degrade them within the lysosomes (Gu et al., 2023; Otero et al., 2006).

Although GPCR endocytosis can occur through several different pathways, the vast majority of GPCRs are internalized by clathrin-mediated endocytosis (CME) (Wolfe and Trejo, 2007). This process relies on the clathrin protein for the formation of vesicular structures from the plasma membrane that later mature into endosomes (Kaksonen and Roux, 2018; Smith and Smith, 2022). While clathrin exhibits a diverse interaction spectrum (Dell'Angelica, 2001; Lemmon and Traub, 2012), it cannot directly interact with the membrane receptors or plasma membrane lipids and requires adaptor proteins to select its internalization cargo (Kovtun et al., 2020; Popova et al., 2013; Smith et al., 1998; Wolfe and Trejo, 2007). The majority of GPCRs require arrestins as endocytic adaptors for internalization (Goodman et al., 1996). The interaction of GPCRs with arrestins is triggered by the phosphorylation of the GPCR C-terminal tail or intracellular loops by GRKs (Gurevich and Gurevich, 2019). Only two non-visual arrestins, arrestin2 and arrestin3, bind to hundreds of non-visual GPCRs (Gurevich and Gurevich, 2019). This is then followed by the interaction with the endocytic machinery (Moo et al., 2021), in particular clathrin (Goodman et al., 1997; Krupnick et al., 1997) and the adaptor complex 2 protein (AP2), which plays a central role in the formation of the clathrin-coated vesicles (Kelly et al., 2014) and the selection of the cargo molecules (Schmid et al., 2006).

We have recently investigated the phosphorylation and arrestin2 interactions of the human chemokine receptor 5 (CCR5) (Isaikina et al., 2023). CCR5 is a GPCR, which acts as the main HIV co-receptor (Alkhatib, 2009) and plays a central role in inflammation (Zeng et al., 2022), COVID-19 infection (Patterson et al., 2021), chronic diseases (Zeng et al., 2022), as well as cancer (Jiao et al., 2019). This revealed a key pXpp GPCR phosphorylation motif in the CCR5 C-terminal tail, which is specifically recognized by well-defined interactions of individual phosphates with positively charged arrestin2 residues. The pXpp motif is widely observed in other receptors (Isaikina et al., 2023; Maharana et al., 2023) known to form a stable complex with arrestin2 (Bous et al., 2022; Huang et al., 2020; Kang et al., 2015). The strength of the arrestin interaction correlates with the phosphosite density and its distribution on the receptor C-terminal tail and intracellular loops (Isaikina et al., 2023; Oakley et al., 2001).

While our previous work revealed the atomic details of the interactions between arrestin and multiple GPCR phosphosites leading to arrestin activation, the interplay between the activated arrestin with clathrin and AP2, which causes receptor internalization, remains poorly understood. Here we have characterized the interactions of arrestin2 with these two proteins as a function of arrestin2 activation by the phosphorylated CCR5 C-terminal tail using NMR and biochemical assays. The results establish strong activation-dependent interactions of arrestin2 with AP2, but not with clathrin. These *in vitro* results are validated by cellular assays, which also demonstrate that CCR5 forms long-lived endocytosed complexes with arrestin2 upon agonist chemokine stimulation.

# Results

## Localizing and quantifying the arrestin2-clathrin interaction by NMR spectroscopy

The CCR5 receptor relies on arrestin2/3 for internalization (Fraile-Ramos et al., 2003) via clathrin-mediated pathways (Signoret et al., 2005). Arrestin2 consists of two consecutive (N-and C-terminal) β-sandwich domains (Figure 1A), followed by the disordered clathrin-binding loop (CBL, residues 353–386), strand β20 (residues 386–390), and a disordered C-terminal tail after residue 393. The CBL contains a clathrin-binding motif ([L/I]ΦXΦ[D/E] where X denotes any amino acid and Φ is a bulky hydrophobic residue (Dell'Angelica, 2001; Smith et al., 2017) (Figure 1A, residues 376–380, Figure 1-figure supplement 1A). Strand β20 forms a characteristic β-sheet with the N-terminal strand β1 in inactive arrestin. Upon activation, the phosphorylated receptor tail replaces β20 in the β-sheet and releases it from the arrestin core.

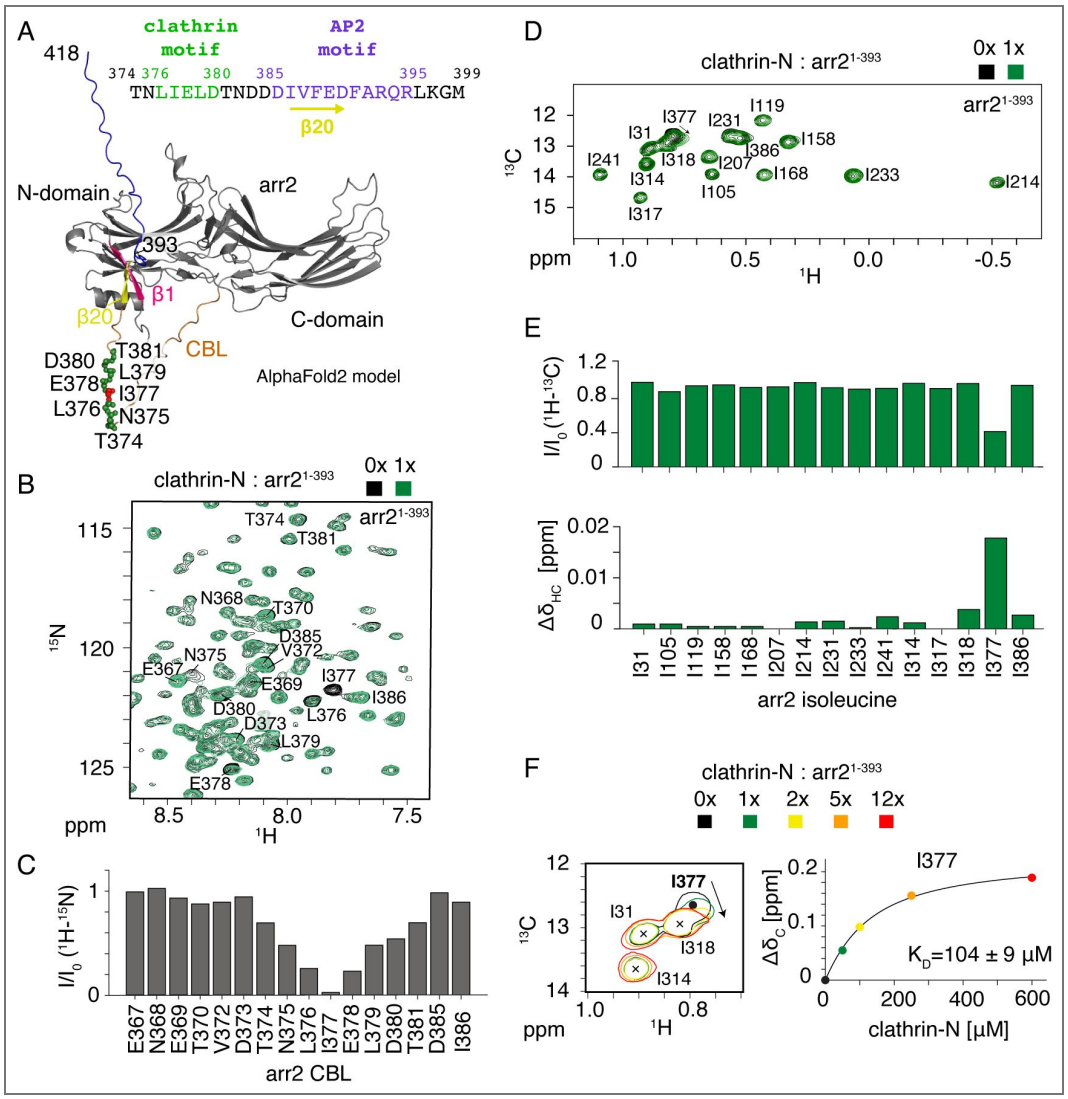


**Figure 1. Arrestin2-clathrin-N interactions detected by arrestin2 NMR spectra.**

(A) AlphaFold2 model of arrestin2$^{1-418}$ (arr2) showing the N- and C-domain (gray) followed by the clathrin-binding loop (CBL, orange), β20 strand (yellow) and the disordered C-terminal tail (blue). The model was used to visualize the clathrin-binding loop and the 344-loop of the arrestin2 C-domain, which are not detected in the available crystal structures of apo arrestin2 [bovine: PDB 1G4M (Han et al., 2001), human: PDB 8AS4 (Isaikina et al., 2023)] due to flexibility. In the other structured regions, the model is virtually identical to the crystal structures. The C-terminal strand β20 forms a parallel β-sheet with the N-terminal strand β1 (pink) in inactive arrestin2 and is released from arrestin2 upon activation by phosphopeptides. Arrestin2 residues interacting with clathrin-N are shown as green (red for main interacting residue I377) spheres. The clathrin and AP2 binding motifs are indicated in the arrestin2 sequence on the top. (B) Part of $^{1}$H-$^{15}$N TROSY spectrum of apo arrestin2$^{1-393}$ (black) and upon addition of an equimolar amount of clathrin-N (green). Assigned CBL arrestin2$^{1-393}$ residues are indicated. (C) Intensity ratios of assigned complexed vs. apo arrestin2$^{1-393}$ CBL resonances. The region between T374 and T381 undergoes significant intensity attenuation. (D) $^{1}$H-$^{13}$C HMQC spectra of apo Ile-δ1-$^{13}CH_3$, $^{2}$H-labeled arrestin2$^{1-393}$ (black) and upon addition of an equimolar amount of clathrin-N (green). (E) Intensity attenuation (top) and chemical shift perturbation (bottom) of arrestin2$^{1-393}$ isoleucine $^{1}H_3$-$^{13}C^{δ1}$ resonances upon clathrin-N addition. Out of 15 isoleucine residues, significant changes are observed only for I377. (F) Left: part of $^{1}$H-$^{13}$C HMQC spectrum showing resonance shifts of I377 upon clathrin-N binding. Right: detected chemical shift changes as a function of clathrin-N concentration. The solid line depicts a non-linear least-square fit to the data points with respective dissociation constant.

Clathrin and arrestin interact in their basal state (Goodman et al., 1996), and a structure of a complex between arrestin2 and the clathrin heavy chain N-terminal domain (residues 1-363, named clathrin-N in the following) has been solved by X-ray crystallography in the absence of an arrestin2-activating phosphopeptide (PDB:3GD1) (Kang et al., 2009). This structure (Figure 1-figure supplement 1B) suggests a 2:1 binding model between arrestin2 and clathrin-N. The first interaction (site I) is observed between the $^{376}$LIELD$^{380}$ clathrin-binding motif of the arrestin2 CBL and the edge of the first two β-sheet blades of clathrin-N, whereas the second interaction (site II) occurs between arrestin2 residues $^{334}$LLGDLA$^{339}$ and the 4th and 5th blade of clathrin-N. The latter arrestin interaction site is not present in the arrestin2 splice variant arrestin2S (for short) where an 8-amino acid insert (residues 334-341) between β-strands 18 and 19 is removed (Kang et al., 2009).

To elucidate the clathrin-arrestin interactions under solution conditions and the influence of arrestin activation we utilized NMR spectroscopy. Figure 1B depicts part of a $^{1}$H-$^{15}$N TROSY spectrum (full spectrum in Figure 1-figure supplement 2A) of the truncated $^{15}$N-labeled arrestin2 construct arrestin2$^{1\text{-}393}$ (residues 1-393), which encompasses the C-terminal strand β20, but lacks the disordered C-terminal tail. Due to intrinsic microsecond dynamics, the assignment of the arrestin2$^{1\text{-}393}$ $^{1}$H-$^{15}$N resonances by triple resonance methods is largely incomplete, but 16 residues (residues 367-381, 385-386) within the mobile CBL could be assigned. This region of arrestin is typically not visible in either crystal or cryo-EM structures due to its high flexibility. The addition of an equimolar amount of clathrin-N (clathrin heavy chain 1, residues 1-364) to arrestin2$^{1\text{-}393}$ induced significant line broadening from residue T374 to T381 with I377 being most strongly affected (Figure 1C, Figure 1-figure supplement 2B). This region almost exactly matches and fully contains the canonical arrestin2 clathrin-binding motif $^{376}$LIELD$^{380}$. Figure 1A shows these interacting residues mapped on an arrestin2 AlphaFold2 model (Jumper et al., 2021).

As $^{1}$H-$^{13}$C methyl resonances have more favorable relaxation properties than backbone $^{1}$H-$^{15}$N resonances (Tugarinov et al., 2003), we used Ile-δ1-$^{13}CH_3$-labeled arrestin2 to quantitatively monitor the formation of the arrestin2-clathrin complex (arrestin2 assignments transferred from BMRB, ID:51131 (Shiraishi et al., 2021)). HMQC spectra of the 15 Ile δ1-$^{13}CH_3$ methyl groups of arrestin2$^{1\text{-}393}$ (Figure 1D) revealed changes in peak intensity (Figure 1E, top) and chemical shift perturbations (Figure 1E, bottom) only for I377 at an equimolar addition of unlabeled clathrin-N to arrestin2$^{1\text{-}393}$. An apparent dissociation constant $K_D$ = 104 ± 9 μM was determined from titrating clathrin-N and fitting the arrestin2 I377 $^{13}$C chemical shifts with a 1:1 binding isotherm (Figure 1F). Although the formed complex (total molecular weight 85 kDa) has low affinity, such interactions are common in endocytosis, which involves many multi-site interactions within a large network of proteins (Smith et al., 2017).

## The arrestin2-clathrin interaction is independent of arrestin2 activation

Due to significant line broadening and peak overlap of the arrestin2 resonances upon phosphopeptide addition, the influence of arrestin activation on the clathrin interaction could not be detected on either backbone or methyl resonances. However, clathrin-N, although similar in size to arrestin2$^{1\text{-}393}$ (41 kDa vs. 44 kDa), provided considerably better $^{1}$H-$^{15}$N TROSY spectra due to the absence of significant micro-to millisecond dynamics. This allowed to observe the effect of arrestin2 activation on its interaction with clathrin by titrating arrestin2$^{1\text{-}393}$ to $^{15}$N-labeled clathrin-N.

Figure 2A (left) shows the intensity changes (full spectra in Figure 2-figure supplement 1A) of the clathrin-N $^{1}$H-$^{15}$N TROSY resonances [assignments transferred from BMRB, ID:25403 (Zhuo et al., 2015)] upon addition of a one-molar equivalent of arrestin2$^{1\text{-}393}$. A significant intensity reduction due to line broadening is detected for clathrin-N residues 39-40, 48-50, 62-72, 83-90, 101-106, and 108. These residues form a clearly defined binding region at the edges of blade 1 and blade 2 of clathrin-N (Figure 2A, right), which corresponds to interaction site I in the 3GD1 crystal structure, involving the conserved arrestin2 $^{376}$LIELD$^{380}$ motif. However, no significant

signal attenuation was observed for clathrin-N residues in blade 4 and blade 5, which would correspond to the crystal interaction site II with arrestin2 residues $^{334}$LLGDLA$^{339}$ that are absent in the arrestin2S splice variant. Thus, only one arrestin2 binding site in clathrin-N is detected in solution, and site II of the crystal structure may be a result of crystal packing.

Next, we tested whether the arrestin2-clathrin-N interaction is enhanced in the presence of the fully phosphorylated CCR5 phosphopeptide (CCR5pp6, where 6 indicates the number of phosphosites, Table S1), which displaces arrestin2 strand β20 by forming an antiparallel β-sheet with strand β1, thereby activating arrestin2 (Isaikina et al., 2023). However, no additional signal attenuation of the clathrin-N $^{1}$H-$^{15}$N resonances or extension to further clathrin-N regions was observed (Figure 2B, Figure 2-figure supplement 1B), when arrestin2$^{1-393}$ was added in the presence of a 5-molar equivalent of CCR5pp6 (corresponding to 80% of arrestin activation). Thus, activation of arrestin2 has apparently no effect on its interaction with clathrin-N. These results suggest that even for receptors with low phosphosite density, such as adrenergic and dopamine receptors (Isaikina et al., 2023; Oakley et al., 2001), the arrestin2-clathrin interaction may still take place allowing efficient receptor internalization.

Previous studies have suggested that the last residues of the arrestin2 C-terminus have an inhibitory effect on clathrin binding (Kern et al., 2009). We therefore tested the interaction of $^{15}$N-labeled clathrin-N with full-length arrestin2 (arrestin2$^{1-418}$). However, the obtained residue intensity attenuation was indistinguishable from the one observed for the arrestin2$^{1-393}$ construct (Figure 2C, Figure 2-figure supplement 1C). Therefore, the residues of the arrestin2 C-terminal tail do not interfere with clathrin binding. In contrast, the interaction of clathrin with arrestin2 (Figure 2D, Figure 2-figure supplement 1D) was completely abolished when the arrestin2 clathrin-binding loop was replaced by the loop of visual arrestin (arrestin2$^{\Delta CBL}$, construct details in Methods). The latter loop lacks the clathrin-binding motif making visual arrestin incapable of interacting with clathrin (Goodman et al., 1997).

Taken together, the solution NMR experiments reveal that arrestin2 interacts with clathrin-N through a single binding site, independently of arrestin2 activation and the conformation of the arrestin2 core.

## Arrestin activation is essential for AP2 interaction

We then proceeded to characterize the interaction of arrestin2 with AP2. AP2 consists of two large (α and β2) and two smaller (μ2 and σ2) subunits (Collins et al., 2002). While each subunit plays a role in CME (Smith et al., 2017), direct recognition of endocytic cargo motifs has been attributed to the σ2 subunit (LL-motif) and μ2 subunit (YxxΦ-motif) (Jackson et al., 2010). The β2 subunit of the AP2 complex (AP2β2) interacts with the arrestin2/3 C-terminus (Kim and Benovic, 2002; Laporte et al., 2002, 2000), and a crystal structure of the complex between the AP2β2 C-terminal domain and a C-terminal arrestin2 peptide (residues 383-402) encompassing strand β20 has been solved (PDB: 2IV8) (Schmid et al., 2006). Interestingly, the C-terminal arrestin2 peptide forms a helical structure in the complex with AP2 (Figure 3A) as opposed to its β-sheet coordination with strand β1 in inactive arrestin2. No experimental data exist on the formation of the AP2-arrestin2 complex in the context of full-length arrestin2 and its activation by phosphorylated receptor tails.

To test how different phosphorylation levels influence arrestin2 recruitment by the C-terminal domain of AP2β2 (AP2β2$^{701-937}$, residues 701-937), we performed a SEC binding assay. In the absence of phosphopeptide an equimolar mixture of 10 μM arrestin2$^{1-418}$ and 10 μM AP2β2 is separated into two peaks (Figure 3B, orange), which elute at the positions corresponding to the individual apo proteins (Figure 3B, blue, green). Upon addition of 100 μM CCR5pp6 (Figure 3C, purple), an additional SEC peak appears at an elution volume of 2.6 ml, which corresponds to the formed arrestin2-AP2β2 complex. Monotonously decreasing complex yields were observed when reducing the amounts of CCR5pp6 added to the mixture (Figure 3D), and no complex formation occurred in the presence of 100 μM non-phosphorylated CCR5 phosphopeptide (CCR5pp0) (Figure 3E). The dissociation constant of the CCR5pp6-arrestin2 complex was determined previously as 45 μM (Table S1) (Isaikina et al., 2023). Not surprisingly, the

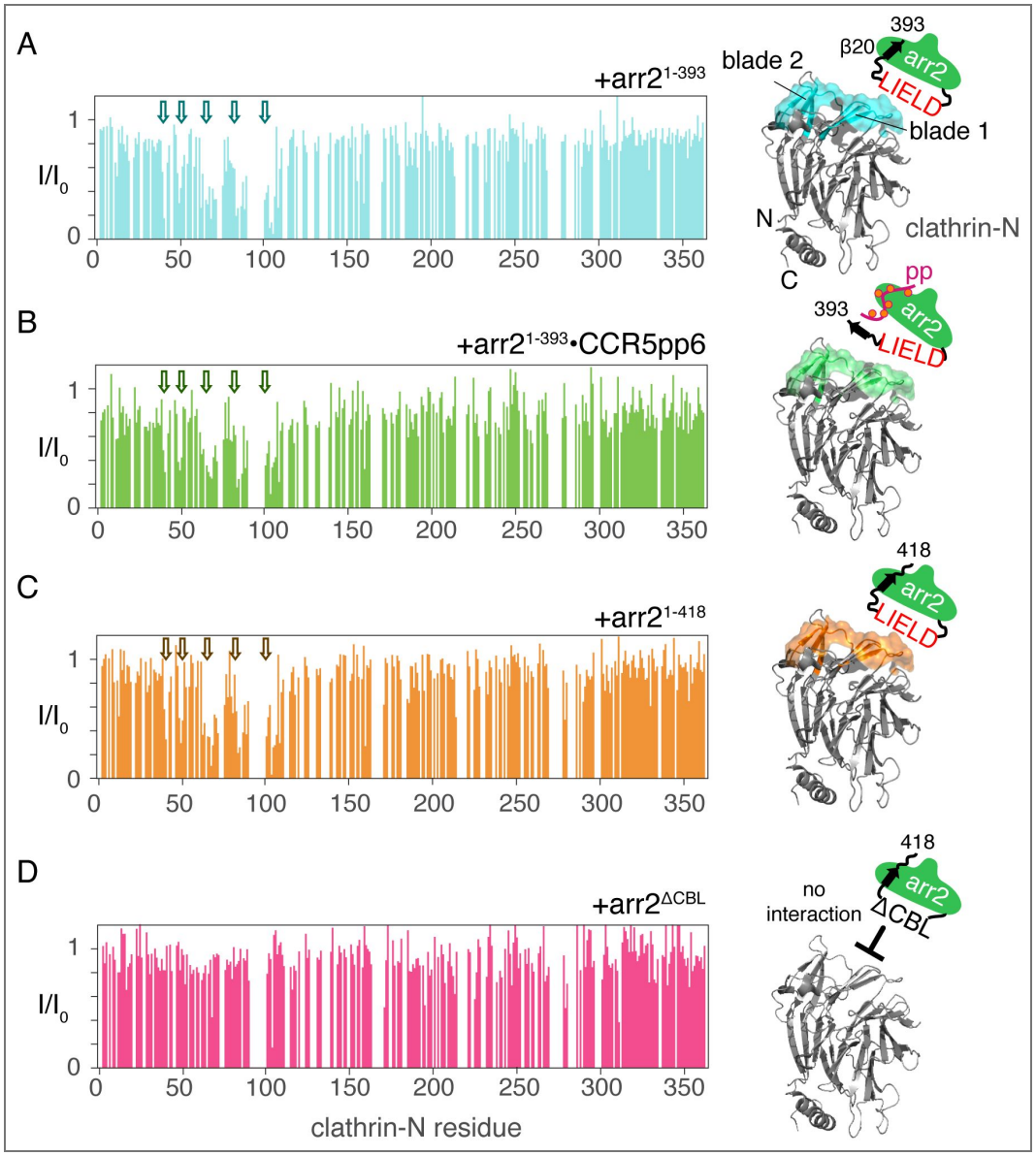


**Figure 2. Arrestin2-clathrin-N interactions detected by clathrin-N NMR spectra.**

(Left): intensity attenuation $I/I_0$ of clathrin-N $^{1}H$-$^{15}N$ TROSY resonances upon addition of equimolar amounts of various arrestin2 constructs: (A) apo arrestin2$^{1-393}$, (B) CCR5pp6-activated arrestin2$^{1-393}$, (C) full-length arrestin2$^{1-418}$ and (D) arrestin2$^{\Delta CBL}$ with removed clathrin-binding motif. Regions that undergo significant attenuation upon interaction with arrestin2 are indicated by arrows. Right: residues undergoing significant intensity attenuation (one standard deviation below the average signal attenuation) are marked on the structure of clathrin-N (PDB: 3GD1) together with a schematic representation of the respective arrestin2 construct.

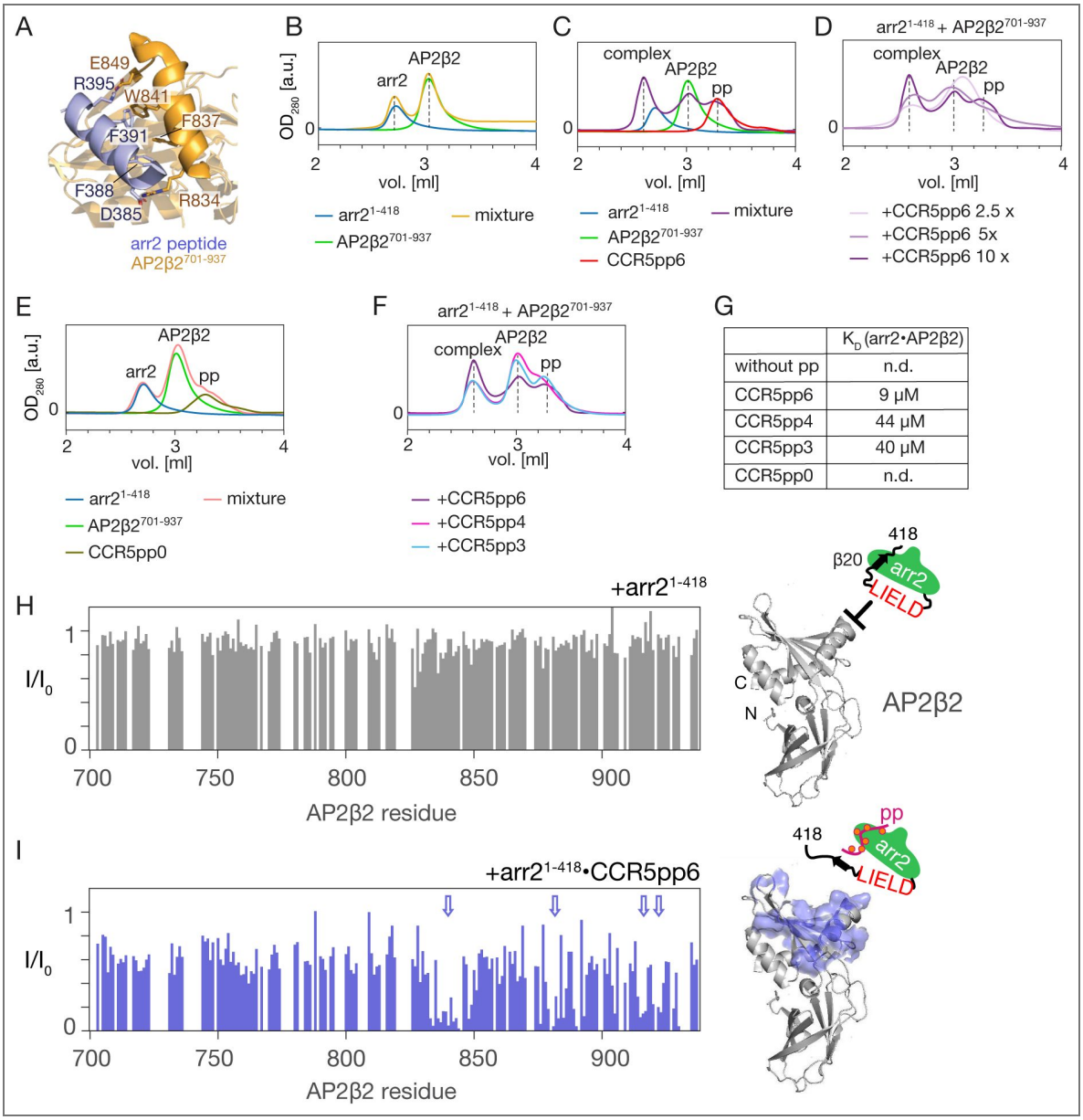


**Figure 3. Arrestin2 interaction with the C-terminal domain of the AP2β2.**

(A) Structure of AP2β2$^{701-937}$ (orange) in complex with arrestin C-terminal peptide (blue) (PDB: 2IV8). Important residues from both chains stabilizing the interaction are depicted in stick representation. (B-F) SEC profiles of arrestin2$^{1-418}$, AP2β2$^{701-937}$, various phosphopeptides and their mixtures. The annotated color coding below the SEC profile indicates the individual sample composition. In panels (B, C, E) 'mixture' refers to a SEC sample containing all of the individual components indicated on the left. In panels (D, F) the primary sample composition is indicated above the SEC profile, and the annotated color coding below the SEC profile indicates the added component to the primary sample composition. (G) Apparent affinities for arrestin2-AP2 complex formation in the presence of phosphopeptides derived by integrating the SEC peaks marked in Figure 4F and scaling the integrals by the respective extinction coefficients. 'nd' indicates 'not detectable'. (H, I) (Left): intensity attenuation $I/I_0$ of AP2β2$^{701-937}$ $^{1}$H-$^{15}$N TROSY resonances upon addition of equimolar amounts of apo arrestin2$^{1-418}$ (H) or CCR5pp6-activated arrestin2$^{1-418}$ (I). Regions that undergo extensive specific attenuation upon interaction with arrestin2 are indicated by arrows. Right: residues undergoing extensive specific intensity attenuation are marked on the structure of AP2β2 (PDB: 2IV8) together with a schematic representation of the respective arrestin2 construct.

formation of the arrestin2-AP2β2 complex depends quantitatively on the affinity of the phosphopeptide-arrestin2 complex. Correspondingly, the addition of the less phosphorylated CCR5pp3 and CCR5pp4 with lower affinities towards arrestin2 (both $K_D$ ~ 200 μM, Table S1) (Isaikina et al., 2023), resulted in a considerable, similar reduction of the formed arrestin2-AP2β2 complex (Figure 4F).

Using the extinction coefficients of all involved polypeptides, the apparent affinities between AP2β2 and arrestin2 could be determined from the SEC profiles (Figure 3G, see Materials and Methods for details). In the presence of 100 μM CCR5pp6, this apparent $K_D$ amounts to 9 μM. An identical affinity value for the affinity between AP2β2 and an isolated arrestin β20 peptide (residues 383-402, D402C) has been observed by EPR spectroscopy (Moaven et al., 2013). In the presence (100 μM) of the less phosphorylated CCR5 peptides, the apparent AP2β2-arrestin2 affinities are reduced by ~4–5 times (CCR5pp4: 44 μM, CCR5pp3: 40 μM), in good agreement with their ~4–5 times reduced affinity for arrestin2.

We also attempted to stabilize the arrestin2-AP2β2-phosphopetide complex through the addition of PIP2, which can stabilize arrestin complexes with the receptor (Janetzko et al., 2022). The addition of PIP2 increased the formation of arrestin2 dimers and higher oligomers, presumably due to the presence of additional charges. Unfortunately, the resolution of the SEC experiments was not sufficient to separate the arrestin2 oligomers from complexes with AP2β2.

It is interesting to note that CCR5pp3 and CCR5pp4 have similar affinities towards arrestin2 despite their different phosphorylation levels (3-fold vs. 4-fold phosphorylated), but only CCR5pp3 contains the pXpp barcode which increases the arrestin2 activation, as assayed by the binding of the Fab30 antibody (Isaikina et al., 2023). Apparently, this barcode does not play a significant role in the formation of arrestin2-AP2β2 complex as the complex formation appears solely governed by the affinity of the phosphopeptide towards arrestin2.

To observe the atomic details of arrestin2 activation on its interaction with AP2β2, we used $^{15}$N-labeled AP2β2$^{701-937}$ [assignment transferred from BMRB ID:52320 (Naudi-Fabra et al., 2024)]. Upon addition of arrestin2$^{1-418}$, no changes in the AP2β2 $^{1}$H-$^{15}$N spectra are detected (Figure 3H, Figure 3-figure supplement 1A), apparently due to the unavailability of arrestin2 β20 strand and C-terminal tail. However, when arrestin2$^{1-418}$ was added in the presence of a 5-molar equivalent of CCR5pp6 (corresponding to 80% of arrestin activation), a significant intensity reduction due to line broadening is detected for many AP2β2 $^{1}$H-$^{15}$N resonances (Figure 3I, left, Figure 3-figure supplement 1B). The strongest attenuated resonances clearly define a binding region within the C-terminal domain of AP2β2 (Figure 3I, right), which is an extension of the binding surface observed in the crystal structure (PDB: 2IV8) of AP2β2 in complex with a 21-residue arrestin2 C-terminal peptide containing strand β20 (Schmid et al., 2006). In agreement with the AP2β2 NMR observations, no interaction was observed in the arrestin2 methyl and backbone NMR spectra upon addition of AP2β2 in the absence of phosphopeptide (Figure 3-figure supplement 1C, D). However, the significant line broadening of the arrestin2 resonances upon phosphopeptide addition (Figure 3-figure supplement 1E, F) precluded a meaningful assessment of the effect of the AP2β2 addition on arrestin2 in the presence of phosphopeptide. The observed line broadening of arrestin2 in the presence of phosphopeptide must be a result of increased protein motions and is not caused by a decrease in protein stability, since the melting temperature of arrestin2 in the absence and presence of phosphopeptide are identical (56.9 ± 0.1 °C).

We then tested whether the presence of clathrin-N influences complex formation between arrestin2 and AP2β2, and vice versa. Arrestin2$^{1-418}$ does not form a complex in the SEC assay with clathrin-N (Figure 3-figure supplement 2A), which agrees with the weak affinity observed in the NMR experiments (Figure 1F). Furthermore, a SEC analysis of a mixture of arrestin2$^{1-418}$, clathrin-N, AP2β2$^{701-937}$, and CCR5pp6 (Figure 3-figure supplement 2B) indicates formation of a complex at 2.6 ml elution volume. An SDS analysis of this complex fraction showed the presence of arrestin2$^{1-418}$ and AP2β2$^{701-937}$, but not of clathrin-N (Figure 3-figure supplement 2C). This indicates that clathrin-N does not interact strongly with the arrestin2-AP2-CCR5 tail complex. As such clathrin may not engage with the initial receptor internalization complex, but may be recruited at later stages of the CME.

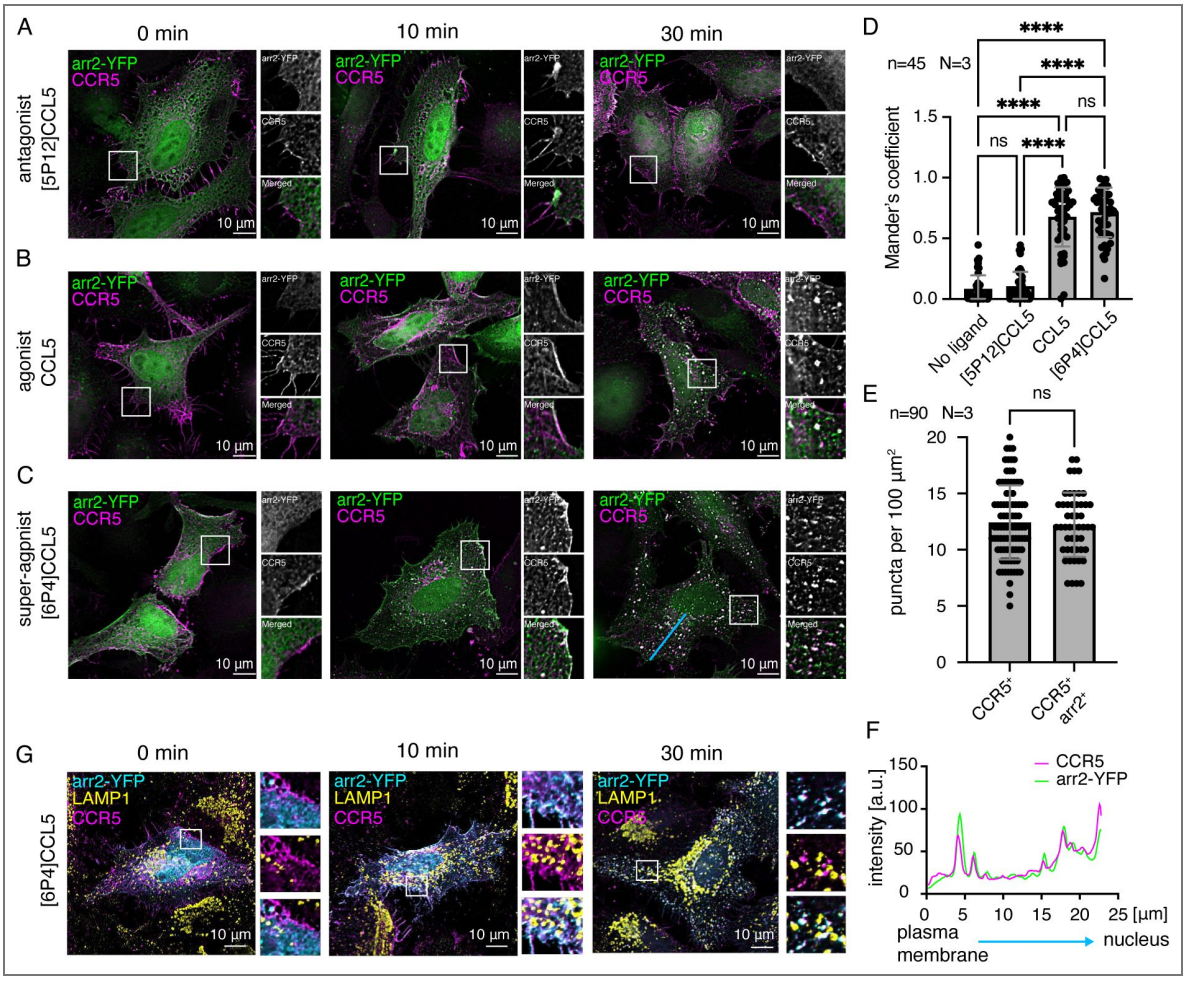


**Figure 4. CCR5 internalization in the presence of the chemokine ligands.**

CCR5 internalization monitored in HeLa cells co-transfected with plasmids containing arrestin2-YFP (green) and CCR5 genes (magenta) stimulated with (A) [5P12]CCL5 (antagonist), (B) CCL5 (natural agonist), (C) [6P4]CCL5 (super-agonist). Cells were stimulated for 0, 10, and 30 min with chemokine ligands before fixation and preparation for fluorescence microscopy. Each image is accompanied by a zoomed region of interest (white squares) showing deconvolved CCR5 and arrestin2-YFP signals. (D) Mander's colocalization coefficients of the CCR5 and arrestin2-YFP signals in the absence and presence of chemokine ligands 30 min after stimulation. Individual values, as well as mean and standard deviation are shown for N=3 biological replicates and n=45 ROIs from 20 cells; ****: $P < 0.0001$; ns: not significant ($P > 0.9999$). (E) Density of CCR5-positive ($CCR5^+$) and CCR5/arrestin2-positive ($CCR5^+$/$arrestin2^+$) puncta after 30 min [6P4]CCL5 ligand stimulation. Individual values, as well as mean and standard deviation are shown for N=3 biological replicates and n=90 ROIs from 30 cells; ns: not significant ($P > 0.9999$). (F) CCR5 and arrestin2 fluorescence signals along the trajectory from the plasma membrane to the nucleus (blue line in panel c) 30 min after [6P4]CCL5 ligand stimulation. (G) Lysosomal trafficking of the CCR5 (magenta) and arrestin2 (cyan) complex in presence of [6P4]CCL5 monitored in the HeLa cells using LAMP1 antibodies (yellow). No recruitment to the lysosome is observed.

To test the stability of the formed arrestin2-AP2 interaction and its quaternary coordination, we performed a trypsin proteolysis assay (Figure 3-figure supplement 3, uncropped gels in Figure 3-figure supplement 4). Trypsin recognizes arrestin2 residue R393 (Xiao et al., 2004), which is buried in the arrestin2 apo state, but is involved in the interaction with AP2β2 (Laporte et al., 2000). Without phosphopeptide, the arrestin2$^{1\text{-}418}$ digestion midpoint occurs at 20-30 min due to the inaccessibility of the cleavage site (Figure 3-figure supplement 3A-C). In the presence of a 5-molar equivalent of CCR5pp6 (Figure 3-figure supplement 3A), the top band corresponding to full-length arrestin2 has almost completely disappeared (relative abundance 19%) already 5 min after incubation as a consequence of the β20 strand release and the exposure of R393 to trypsin. However, the presence of AP2β2$^{701\text{-}937}$ protects arrestin$^{1\text{-}418}$ from proteolysis, as evident from significantly higher abundance at 5 min and a shift of the proteolysis midpoints to 10, 20, and 30 min at 1-, 2-, and 5-molar equivalents of AP2β2$^{701\text{-}937}$ respectively.

Analogous digestion experiments using CCR5pp3 (Figure 3-figure supplement 3B) or CCR5pp4 (Figure 3-figure supplement 3C) phosphopeptides revealed that they did not enhance the rate of arrestin2 proteolysis by trypsin at a 3-molar equivalent, as expected from their weaker affinity towards arrestin2. In agreement with this, however, upon addition of 25-molar equivalents of either peptide the rate of arrestin2 proteolysis was significantly increased, as full-length arrestin2 almost completely disappeared already 5 min after incubation. Thus as for CCR5pp6, the presence of AP2β2$^{701\text{-}937}$ also protects arrestin2$^{1\text{-}418}$ activated by CCR5pp3 or CCR5pp4 from proteolysis.

In summary, these results indicate that arrestin2 activation by the binding of receptor phosphopeptides and the subsequent release of its strand β20 is required for the interaction with AP2. This interaction is modulated by the phosphorylation level of the receptor C-terminal peptide and its relative abundance. The formed AP2 complex with arrestin is stable and more resistant to proteolysis.

## Ligand-dependent CCR5 internalization monitored in HeLa cells

We then validated the obtained *in vitro* results on the CCR5-arrestin2-clathrin and -AP2 interactions by cellular assays. According to the strength and persistence of arrestin interactions, GPCRs have been categorized into class A and class B subtypes (Isaikina et al., 2023; Oakley et al., 2000). To distinguish these arrestin classes from the common IUPHAR classification of GPCRs, we refer in the following to them as arr-class A and B, respectively. Arr-class A receptors (e.g. adrenergic receptors) form transient complexes with arrestins that quickly dissociate near the plasma membrane and the receptor traffics alone into endosomes. In contrast, arr-class B receptors (e.g. the vasopressin receptor 2, V2R) have a higher affinity towards arrestin and form long-lived complexes that traffic together into endosomes (Oakley et al., 2000). We have recently established that the phosphorylated CCR5 C-terminus forms a high-affinity complex with arrestin (Isaikina et al., 2023), thus assigning the CCR5 to the arr-class B subtype.

To better understand the stability of CCR5-arrestin2 complex, we first monitored CCR5 internalization upon chemokine stimulation in fixed HeLa (CCL2, ATCC nomenclature) cells (Figure 4). HeLa cells were transiently transfected with plasmids containing C-terminally FLAG-tagged CCR5 and YFP-tagged arrestin2 (arrestin2-YFP) genes. This receptor construct was used to minimize CCR5 modifications and monitor the arrestin2 interaction in conditions as close to native as possible. Before the addition of the chemokine ligands (0 min), CCR5 was observed at the plasma membrane (magenta), while arrestin2 (green) was distributed throughout the cell (Figure 4A-C). Cells stimulated with the antagonist chemokine [5P12]CCL5 (Gaertner et al., 2008) retained this CCR5 and arrestin2 distribution even 30 min after ligand addition (Figure 4A). In contrast, when cells were stimulated with the native agonist chemokine CCL5 (Hughes and Nibbs, 2018) (Figure 4B) or the super-agonist [6P4]CCL5 (Gaertner et al., 2008; Isaikina et al., 2021) (Figure 4C), recruitment of arrestin2 from the cytoplasm to the plasma membrane could be detected within 10 min. Prolonged ligand incubation times (30 min) lead to CCR5 internalization in complex with arrestin2. To eliminate the possibility that arrestin2 recruitment to the membrane was due to interactions with endogenous proteins in HeLa cells, we monitored internalization in live cells transfected only with arrestin2. In this case, the cells did not show

characteristic arrestin2 recruitment to the plasma membrane or robust puncta formation, indicative of endosomes, even in the presence of the super-agonist (Figure 4-figure supplement 1A). This control experiment also revealed a few internal arrestin puncta devoid of receptor, presumably due to the arrestin2 overexpression. This phenomenon was also observed previously (Beautrait et al., 2017; Oakley et al., 2000).

Stronger phosphorylation and arrestin2/3 recruitment potencies have been reported for [6P4]CCL5 as compared to wild-type CCL5 (Martins et al., 2020). In agreement with this, [6P4]CCL5 appears more potent than CCL5 in recruiting arrestin2 to the plasma membrane and inducing CCR5-arrestin2 puncta formation after 10 min (Fig 4B, C). However, 30 min after stimulation, no significant difference in CCR5 and arrestin2 colocalization was observed as quantified by the Mander's coefficient (Figure 4D). The Mander's coefficient is about 0.7 in cells stimulated by either agonist, but close to zero for non-stimulated or antagonist-incubated cells (Figure 4D). Apparently the two agonist ligands induce a differing initial rate of arrestin2 recruitment by CCR5. However, once arrestin2 is recruited, the CCR5-arrestin2 complex accumulates and remains stable for at least 30 min inside the cells.

To further corroborate the arr-class B-like behavior of CCR5, we counted the puncta positive for CCR5 or both CCR5 and arrestin2 in cells at this time point after stimulation by [6P4]CCL5 (Figure 4E). No significant difference was observed between the two values. This indicates that the number of puncta containing only CCR5, but not arrestin2, must be very small and that the majority of CCR5 puncta also contains arrestin2, consistent with stable complex formation. Furthermore, the CCR5 and arrestin2 colocalization occurs not only close to the plasma membrane but also close to the nucleus (Figure 4F), indicative of the arr-class B-like behavior of CCR5. For arr-class A receptors, it would be expected that arrestin2 is excluded from receptor-containing structures, which traffic into the perinuclear region (Oakley et al., 2000).

As both recycling (Gu et al., 2023; Mueller et al., 2002) and degradation (Gu et al., 2023) has been observed during CCR5 internalization, the cellular fate of the CCR5-arrestin2 complex was probed using the lysosomal-associated membrane protein 1 (LAMP1) as a marker of the lysosomal membranes (Figure 4G). No recruitment of the complex to the lysosomes (LAMP1, yellow) was detected in the presence of [6P4]CCL5 even 30 min after ligand stimulation. Similar results were obtained for both CCL5 and [6P4]CCL5 in live cells using the LysoTracker$^{TM}$ dye that accumulates in acidic environments, such as the lysosome (Figure 4-figure supplement 1B, C). These results indicate that the CCR5 internalization pathway, although mediated by arrestin, does not lead to rapid receptor degradation in lysosomes.

## Arrestin interaction with AP2 is essential for CCR5 internalization

The interactions of arrestin with clathrin and AP2 have mostly been studied for the internalization of the β2-adrenergic (β2AR) (Barsi-Rhyne et al., 2022; Beautrait et al., 2017; Goodman et al., 1996; Kang et al., 2009; Kim and Benovic, 2002) and V2R (Barsi-Rhyne et al., 2022; Beautrait et al., 2017) receptors. Here, we investigated how both interactions affect the internalization of CCR5 in a HeLa KO cell line (HeLa$^{-arr2/3}$) devoid of arrestin2 and arrestin3 as well as in HeLa (CCL2) cells (Figure 5, Figure 5-figure supplement 1, respectively).

To characterize the arrestin2-clathrin interaction, we generated a YFP-tagged arrestin2 construct with the clathrin-binding motif (arrestin2$^{\Delta LIELD}$-YFP) removed. No significant difference in CCR5 internalization was detected in either HeLa cell line between wild-type arrestin2-YFP and arrestin2$^{\Delta LIELD}$-YFP, when the cells were stimulated with [6P4]CCL5 (HeLa$^{-arr2/3}$: Figure 5A-C, HeLa: Figure 5-figure supplement 1A). Apparently, the arrestin2-clathrin interaction does not play a significant role in the internalization of the arr-class B CCR5 receptor. This is in contrast to findings for the arr-class A receptor β2AR where removal of the LIELD motif impairs receptor internalization (Kim and Benovic, 2002).

To test the influence of the arrestin2-AP2 interaction, we introduced mutations within the arrestin2 adaptin-binding motif, which is conserved across all arrestins (Figure 1-figure supplement 1A). The mutation R395A within this motif has been found to inhibit β2AR

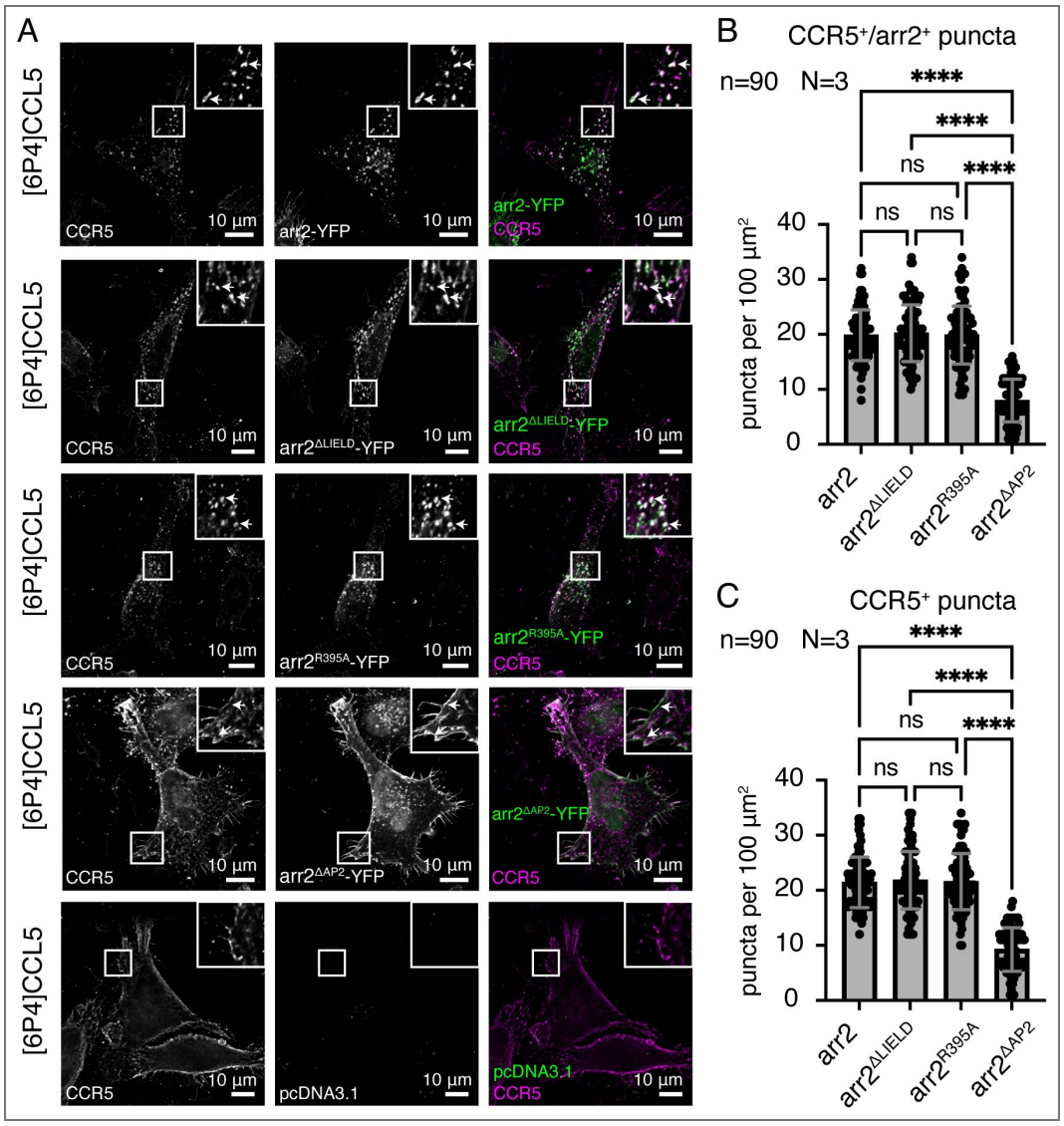


**Figure 5. Dependence of CCR5 internalization on arrestin2 interactions with clathrin or AP2 monitored in HeLa$^{-arr2/3}$ cells.**

(A) CCR5 internalization induced by 60 min [6P4]CCL5 ligand stimulation in HeLa cells co-transfected with plasmids containing CCR5 and arrestin2-YFP, arrestin2-YFP$^{\Delta LIELD}$, arrestin2-YFP$^{R395A}$, arrestin2-YFP$^{\Delta AP2}$ or empty pcDNA3.1. (B, C) Internalization was quantified by counting the number of puncta (B) positive for CCR5 and arrestin2 (CCR5$^{+}$/arrestin2$^{+}$) or (C) only CCR5$^{+}$ 60 min after ligand stimulation in the HeLa$^{-arr2/3}$ cells. No significant difference in CCR5 internalization is detected for the arrestin2-YFP$^{\Delta LIELD}$ and arrestin2-YFP$^{R395A}$ constructs (ns, not significant: $P > 0.9999$) whereas the absence of the AP2 binding motif in the arrestin2$^{\Delta AP2}$-YFP construct causes a significant (****: $P < 0.0001$) reduction of CCR5 internalization 60 min after ligand incubation. Mean and standard deviation are shown for N=3 biological replicates and n=90 ROIs from 30 cells.

internalization by arrestin3 (Laporte et al., 2000). Introducing the equivalent mutation into a fluorescent arrestin2 construct (arrestin2$^{R395A}$-YFP), did not lead to significant changes in CCR5 internalization relative to wild-type arrestin2-YFP (HeLa$^{-arr2/3}$: Figure 5A-C, HeLa: Figure 5-figure supplement 1B).

The structure of AP2β2 in complex with the C-terminal arrestin2 peptide (Schmid et al., 2006) shows arrestin2 residues D385, F388, F391, and R395 interacting via salt bridges and base stacking with AP2β2 (Figure 3A). Apparently, these interactions lead to a rather stable complex of full-length arrestin2 with AP2β2$^{701-937}$ in solution as evidenced by our SEC binding assay, NMR and the protection of activated arrestin2 against proteolysis (Figure 3, Figure 3-figure supplement 3). We hypothesized that due to this extended arrestin2-AP2β2 interaction interface, the mutation of a single interacting residue may not suffice to inhibit the arrestin2-AP2 interaction leading to CCR5 internalization. Hence, we generated a further arrestin2 mutant (arrestin2$^{\Delta AP2}$-YFP) with all four direct interacting residues replaced (D385A, F388A, F391A, R395A). Similar to wild-type arrestin2-YFP, arrestin2$^{\Delta AP2}$-YFP is recruited to CCR5 at the plasma membrane (HeLa: Figure 5-figure supplement 1C). However, the subsequent CCR5 internalization is potently inhibited (HeLa$^{-arr2/3}$: Figure 5A-C, HeLa: Figure 5-figure supplement 1D) as indicated by a reduction of the Mander's CCR5/arrestin2 colocalization coefficient (from ~0.8 to ~0.2) the number of puncta positive for CCR5 and arrestin2 (from ~20–13 to ~8–6 per 100 μm$^2$, similar values obtained for CCR5 puncta). In agreement with this finding, the arrestin2$^{\Delta AP2}$ mutant is unable to form a complex with AP2 in the presence of CCR5pp6 as assayed by SEC (Figure 5-figure supplement 1E). Taken together, these results show that the stable arrestin-AP2 interaction is crucial for CCR5 internalization, whereas the arrestin-clathrin interaction is not critical for sequestration from the plasma membrane.

# Discussion

In the present study, we have elucidated the role of CCR5 phosphorylation in arrestin-clathrin and arrestin-AP2 interactions which are essential for CCR5 sequestration into cells. NMR and chromatographic data on arrestin2 interactions with clathrin and AP2 proteins in the presence of arrestin2-activating CCR5 C-terminal phosphopeptides revealed the molecular details underlying CCR5 sequestration. Whereas the analysis of arrestin2 $^{1}$H-$^{15}$N resonances was difficult due to significant line broadening from intrinsic microsecond dynamics (Isaikina et al., 2023), the better quality of the clathrin-N $^{1}$H-$^{15}$N spectra allowed a detailed characterization of the arrestin2-clathrin interaction from the clathrin side. Arrestin2 binds to clathrin with about 100 μM affinity. This interaction is independent of arrestin2 activation by phosphopeptides, which may enable the internalization of receptors with low phosphorylation levels. The interaction is mediated through a single binding site in a 1:1 stoichiometry involving the arrestin2 clathrin-binding loop and the edges of blade 1 and blade 2 of clathrin-N. This binding site agrees with one of the binding sites observed in the crystal structure of the arrestin2-clathrin-N complex (PDB: 3GD1), but disagrees with the second crystal interaction site involving the arrestin2 splice loop. Presumably, the latter is a result of crystal packing. Our findings are supported by a previous study (Lally et al., 2017), which suggests that the arrestin C-domain edge containing the splice loop anchors arrestin to the membrane. The membrane anchoring seems mutually exclusive with clathrin binding (Lally et al., 2017).

In contrast to the arrestin2-clathrin interaction, the arrestin2-AP2 interaction requires arrestin2 activation by GPCR C-terminal tail phosphopeptides and depends quantitively on their phosphorylation levels. The formed arrestin2-phosphopeptide-AP2 complexes are stable and more resistant to proteolysis than binary arrestin2-phosphopeptide complexes. The dissociation constant of the arrestin2-AP2 complex is about 10 μM in the presence of the fully phosphorylated CCR5pp6, which is a 10-fold higher affinity than that of the arrestin2-clathrin complex. This may indicate a preference towards AP2 complex formation for highly phosphorylated receptors. However, as the phosphorylation decreases the arrestin2-AP2 dissociation constant weakens to about 40 μM, making it more comparable to the arrestin2-clathrin interaction.

Cellular experiments demonstrated chemokine agonist-induced recruitment of arrestin2 towards CCR5 at the plasma membrane, which is followed by the sequestration of the CCR5-arrestin2 complex into the cytoplasm including the perinuclear region where it remains stable for an extended period. This provides experimental evidence that CCR5 belongs to the arr-class B of GPCRs as surmised previously from the large number of phosphorylation sites in its C-terminus and the presence of the pXpp motif (Isaikina et al., 2023). The sequestered receptor remained stable inside the cells for at least 30 min, and was not rapidly degraded in lysosomes, even in the presence of [6P4]CCL5. A similar CCR5 lysosome-evading internalization pattern has been observed for the potent anti-HIV chemokine analog PSC-RANTES (Escola et al., 2010). As a recent CCR5 trafficking study demonstrated that CCR5 scavenges both CCL5 and [6P4]CCL5 chemokines in an arrestin-dependent manner (Gu et al., 2023), it is possible that the long retention of the CCR5-arrestin complex and the ability of the receptor to undergo recycling (Gu et al., 2023; Mueller et al., 2002) is utilized to remove the extracellular ligands from the cell surface. This may help in the regulation of chemokine ligand concentrations (Ariel et al., 2006).

Based on the present CCR5 data, we envision the following CME mechanism, which may also apply to other arr-class B receptors (Figure 6, left). The high receptor phosphorylation leads to a strong recruitment of arrestin even in the absence of interactions with negatively charged $PIP_2$ in the plasma membrane (Janetzko et al., 2022). The consequent tight binding of the phosphorylated receptor tail to arrestin strand β1 stably activates arrestin thereby releasing its strand β20 and C-terminal tail. The freed β20 strand can then interact with the β2 subunit of AP2, which becomes released from the AP2 core upon AP2 activation by $PIP_2$ molecules (Kelly et al., 2014). Apparently, the interaction of arrestin2 strand β20 with the AP2 β2 subunit is rather strong, since it could only be inhibited in cellular assays by a fourfold, but not by a single mutation in the arrestin2 C-terminal region. In contrast, removal of the clathrin-binding LIELD motif from arrestin2 did not impair receptor internalization, which is in agreement with the determined relatively low affinity of the arrestin2-clathrin interaction. This suggests that the clathrin interaction is less important for receptor internalization than the AP2 interaction.

The AP2 activation by $PIP_2$ also exposes the AP2 clathrin-binding LLNLD motif, responsible for clathrin recruitment and formation of the clathrin-coated pits (Kelly et al., 2014). In the stable ternary complex of a highly phosphorylated arr-class B receptor with arrestin and AP2, the exposed AP2 LLNLD clathrin-binding motif may then subsequently couple to the clathrin network thereby inducing rapid sequestration from the plasma membrane into endosomes. The direct clathrin interaction of arrestin via its LIELD motif appears less important in this respect.

Although the generalization of this mechanism from CCR5 to other arr-class B receptors has to be explored further, it is indirectly corroborated in the visual rhodopsin-arrestin1 system. The arr-class B receptor rhodopsin (Isaikina et al., 2023) also undergoes CME (Moaven et al., 2013) with arrestin1 harboring the conserved AP2 binding motif, but missing the clathrin-binding motif (Figure 1-figure supplement 1A). As arr-class B receptors are almost all peptide-binding GPCRs (Isaikina et al., 2023; Oakley et al., 2000), we speculate that the strong arrestin interaction may also be utilized to remove the extracellular ligands from the plasma membrane, independent of receptor degradation.

In comparison to arr-class B receptors, arr-class A receptors have a lower phosphosite density in their C-terminal tails. Previous studies on the arr-class A β2AR (Kang et al., 2009; Kim and Benovic, 2002; Laporte et al., 2000) revealed that both clathrin and AP2 interaction are crucial for internalization. It is expected that the lower phosphosite density of arr-class A receptors results in a less stable interaction with arrestin (Figure 6, right). Therefore additional interactions with $PIP_2$ lipids are required to anchor arrestin to the membrane and play a significant role in receptor endocytosis (Janetzko et al., 2022). As a consequence of the low phosphorylation of the receptor and the weakened interaction with arrestin strand β1, the equilibrium between inactive (strand β20 forms β-sheet with β1) and active (β20 released) arrestin is shifted towards the inactive conformation, even when arrestin is bound to the receptor via core contacts. Due to the low availability of strand β20, the arrestin interaction with AP2 is considerably weakened and comparable in strength to the clathrin interaction. This is consistent

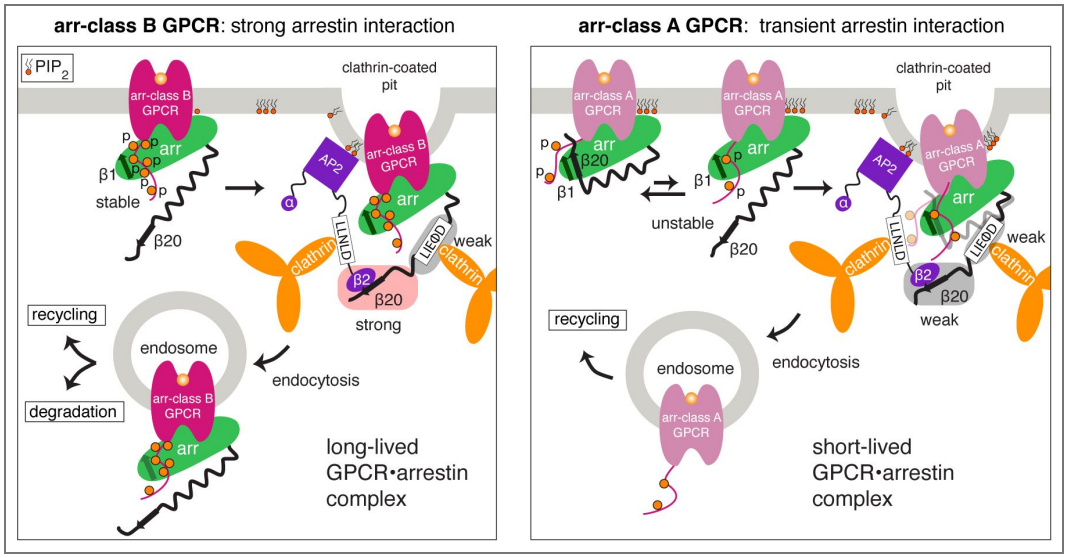


**Figure 6. Overall scheme of arr-class A and B GPCR internalization.**

Schematic difference of arrestin2-mediated internalization of arr-class B (left) vs. arr-class A (right) GPCRs. Arr-class B GPCRs bind stably to arrestin due to their high levels of phosphorylation. This results in a robust release of the arrestin C-terminus, a stable interaction with AP2 and formation of a long-lived GPCR•arrestin complex. Arr-class A GPCRs bind weakly to arrestin due to their poor phosphorylation. They require stabilization of the arrestin complex by membrane-bound $PIP_2$ molecules. The arrestin C-terminus is not fully released and consequently the interaction with AP2 is unstable.

with the finding that AP2 and clathrin participate with similar strength in arr-class A receptor internalization (Kang et al., 2009; Kim and Benovic, 2002; Laporte et al., 2000). However, as both interactions are weak, the sequestration is reduced. In addition, the weaker receptor phosphorylation leads to fast dissociation of arrestin from the receptor at or near the plasma membrane, and in consequence the receptor traffics without arrestin into endosomes (Oakley et al., 2001, 2000).

In conclusion, this biophysical and cellular analysis of the interactions between the CCR5, arrestin2, and clathrin/AP2 endocytic machinery elucidates the interplay of molecular forces driving GPCR internalization. The strength of the receptor phosphorylation modulates the interaction with arrestin2, the release of its strand β20, and subsequently its interaction with the β2 subunit of AP2. In comparison, the arrestin2-clathrin interaction is weaker. The interaction between the receptor phosphosites and arrestin appears as a distinctive factor between arr-class B and arr-class A receptor sequestration, since phosphorylation of the latter is considerably weaker. These findings expand on the previously suggested mechanism for the reduced sequestration of the arr-class A receptor β2AR by Kim and Benovic (Kim and Benovic, 2002) and Laporte et al (Laporte et al., 2000), where the weakened AP2-arrestin and the phosphorylation-independent clathrin-arrestin interactions appear of similar importance. The phosphorylation dependence of the AP2-arrestin interaction may also play a role in modulating the strength of downstream arrestin-mediated signaling from endosomes (Jean-Charles et al., 2017; Tohgo et al., 2003). A detailed understanding of these molecular interactions may provide a framework for the development of novel therapeutics interfering with GPCR sequestration.

# Materials and methods

## Constructs

The genes encoding full-length (arrestin2$^{1\text{-}418}$) and truncated (arrestin2$^{1\text{-}393}$) human arrestin2 constructs have been described before (Isaikina et al., 2023). The arrestin2$^{\Delta CBL}$ construct in a pET-28a (+) vector was obtained from the GenScript by replacing the loop residues of arrestin2 K357 to D385 with visual arrestin residues E365 to N376. The construct also contained an N-terminal hexahistidine tag for purification followed by a TEV cleavage site (ENLYFQG), resulting in the following total sequence (arrestin2$^{\Delta CBL}$ in bold, visual arrestin loop underlined):

MGSSHHHHHHSSGENLYFQG**MGDKGTRVFKKASPNGKLTVYLGKRDFVDHIDLVDPVDGVVLVDPEY LKERRVYVT**
**LTCAFRYGREDLDVLGLTFRKDLFVANVQSFPPAPEDKKPLTRLQERLIKKLGEHAYPFTFEIPPNLPC SVTLQPG**
**PEDTGKACGVDYEVKAFLAENLEEKIHKRNSVRLVIRKVQYAPERPGPQPTAETTRQFLMSDKPLHLE ASLDKEIY**
**YHGEPISVNVHVTNNTNKTVKKIKISVRQYADIVLFNTAQYKVPVAMEEADDTVAPSSTFSKVYTLTPF LANNREK**
**RGLALDGKLKHEDTNLASSTLLREGANREILGIIVSYKVKVKLVVSRGGLLGDLASSDVAVELPFTLM HPKPEDPA KESYQDANIVFEDFARQRLKGMKDDKEEEEDGTGSPQLNNR**

clathrin-N [pETM33_CLTC_Clathrin propeller, clathrin heavy chain 1 residues 1-364, Addgene plasmid #178471 (Benz et al., 2022)] and AP2β2$^{701\text{-}937}$ [pETM33_AP2B1_adaptin, Addgene plasmid #178467 (Benz et al., 2022)] constructs were gifts from Ylva Ivarsson. Arrestin2-YFP was a gift from Robert Lefkowitz [Addgene plasmid # 36916, (Violin et al., 2006)].

The arrestin2$^{\Delta LIELD}$-YFP construct was obtained from the arrestin2-YFP template by standard PCR reaction using KAPA HiFi polymerase (forward primer: 5'-GAG ACT CCA GTA GAC ACC AAT ACC AAT GAT GAC GAC A-3'; reverse primer: 5'-TGT CGT CAT CAT TGG TAT TGG TGT CTA CTG GAG TCT C-3').

Arrestin2$^{R395A}$-YFP was generated in the same manner using forward primer: 5'-GGA CTT TGC TCG TCA GGC GCT GAA AGG CAT GAA G-3' and reverse primer: 5'-CTT CAT GCC TTT CAG CGC CTG ACG AGC AAA GTC C-3'.

The same protocol was applied for generating the arrestin2 $^{\Delta AP2}$-YFP clone with the forward primer 5'-GAC ACC AAT GAT GAC GCC ATT GTG GCT GAG GAC GCT GCT CGT CAG GCG CTG AAA GGC ATG-3' and reverse primer 5'-CAT GCC TTT CAG CGC CTG ACG AGC AGC GTC CTC AGC CAC AAT GGC GTC ATC ATT GGT GTC-3'.

The CCR5 construct in pcDNA3.1 used in cellular assays was obtained from GenScript. The complete construct contained the full-length human CCR5 sequence (bold) followed by a GS-linker and a C-terminal FLAG-tag (underlined):

**MDYQVSSPIYDINYYTSEPCQKINVKQIAARLLPPLYSLVFIFGFVGNMLVILILINCKRLKSMTDIYLLN LAISD**
**LFFLLTVPFWAHYAAAQWDFGNTMCQLLTGLYFIGFFSGIFFIILLTIDRYLAVVHAVFALKARTVTFG VVTSVIT**
**WVVAVFASLPGIIFTRSQKEGLHYTCSSHFPYSQYQFWKNFQTLKIVILGLVLPLLVMVICYSGILKTLL RCRNEK**
**KRHRAVRLIFTIMIVYFLFWAPYNIVLLLNTFQEFFGLNNCSSSNRLDQAMQVTETLGMTHCCINPIIY AFVGEKF**
**RNYLLVFFQKHIAKRFCKCCSIFQQEAPERASSVYTRSTGEQEISVGL**GSGGGGSGGSSSGGGGSGGSSSG GEFDY KDDDDK

The genes encoding [5P12]CCL5 (Wiktor et al., 2013), CCL5 (Wiktor et al., 2013) and [6P4]CCL5 (Isaikina et al., 2022) for expression in *E. coli* have been described previously.

## Protein expression and purification

All protein constructs were expressed in *E. coli* BL21 (DE3) cultured in Lysogeny broth medium (LB). For the preparation of the deuterated $^{15}$N-labeled (and $^{13}$C-labeled) NMR samples, cells were grown in $D_2O$/$^{15}NH_4Cl$ ($^{13}$C-glucose) M9 minimal medium. For the preparation of Ile-δ1-$^{13}CH_3$-labeled arrestin2$^{1\text{-}393}$, the minimal medium was supplemented with 80 mg per liter of 2-ketobutyric acid-4-$^{13}$C,3,3-$d_2$ sodium salt hydrate following previously reported procedures (Tugarinov et al., 2006). In all cases, cells were grown at 37°C until the optical density at 600 nm ($OD_{600\ nm}$) reached 0.7–0.8. Thereafter protein expression was induced by the addition of 25 μM isopropyl β-D-thiogalactopyranoside (IPTG) (arrestin2 constructs) or 1 mM IPTG (clathrin-N and AP2β2$^{701\text{-}937}$). The temperature was lowered to 18°C (arrestin2 constructs) or 22°C (clathrin-N and AP2β2$^{701\text{-}937}$) for an overnight expression, after which the cells were harvested by centrifugation (30 min at 6000 rpm).

### Arrestin2

The purification of arrestin2 has been described before (Isaikina et al., 2023). In short, arrestin2$^{1\text{-}418}$, arrestin2$^{1\text{-}393}$, arrestin2$^{\Delta CBL}$ and arrestin2$^{\Delta\Delta P2}$ were purified on a Ni-NTA HiTrap HP column (GE Life Sciences) and the His-tag was removed by overnight cleavage with TEV protease (homemade). The cleaved protein was further separated from impurities by a reverse IMAC step on a Ni-NTA HiTrap HP column. An ion exchange chromatography step using a 5-ml HiTrap Q HP anion exchange column was then carried out before the final gel filtration step on a HiLoad 16/600 Superdex 200 pg gel filtration column (GE Healthcare) equilibrated with 20 mM HEPES, 150 mM NaCl, pH 7.4 (SEC buffer I). Protein purity was confirmed by SDS-PAGE.

### clathrin-N

clathrin-N was purified similarly to the arrestin2 protocol using a Ni-NTA HiTrap HP column. The His-tag was removed by overnight cleavage with 3C protease (homemade), followed by a reverse IMAC step. The protein was concentrated in a Vivaspin 20 (Sartorius) concentrator (10-kDa MWCO) before a final gel filtration step on a HiLoad 16/600 Superdex S75 pg gel filtration column (GE Healthcare) equilibrated with SEC buffer I. Protein purity was confirmed by SDS-PAGE.

### AP2β2

AP2β2 was purified similarly to clathrin-N. Due to a change of the isoelectric point from 6.6 to 7.7 after 3C protease cleavage, the pH of the SEC buffer was changed to 7.0 (SEC buffer II, 20 mM HEPES, 150 mM NaCl, pH 7.0).

### Determination of protein melting temperature

Protein melting temperatures were determined routinely by differential scanning fluorimetry using a Prometheus Nanotemper NT.48 (Tecan) instrument.

## Peptide synthesis

Phosphorylated peptides (Table S1) corresponding to the last 22 residues of the human CCR5 receptor (CCR5pp3, CCR5pp4, CCR5pp6) were obtained from the Tufts University Core Facility for peptide synthesis.

## Cell culture

HeLa (ATCC CCL2) cells and HeLa KO cell line (HeLa$^{-arr2/3}$) (D'Agostino et al., 2020) devoid of arrestin2 and arrestin3 were grown in high-glucose Dulbecco's modified Eagle's medium (Sigma-Aldrich) with 10% fetal bovine serum (FBS, Biowest), 2 mM L-glutamine (#25030; Gibco), 100 U ml$^{-1}$ penicillin G and 100 ng ml$^{-1}$ streptomycin (P433; Sigma-Aldrich Chemie GmbH), 1 mM sodium pyruvate (#S8636; Sigma-Aldrich Chemie GmbH) at 37°C and 5% $CO_2$. For transient cell transfections, cells were plated into six-well plates to reach 70% confluency the following day and transfected with 0.3 µg of each arrestin2-YFP and CCR5 plasmid DNA complexed with Helix-IN transfection reagent (OZ Biosciences).

## Immunostaining and microscopy

In HeLa cell lines, arrestin2 and CCR5 were overexpressed by transiently transfecting arrestin2-YFP and CCR5 respectively. CCR5 was stained with a primary FLAG antibody (1:200, Thermo Fisher F3165) in 5% FBS in PBS. A secondary mouse (1:500) Alexa 633 (A21052, Invitrogen) antibody was used in 5% FBS in PBS. Fluoromount-G mounting medium (Thermo Fischer) was used to mount the coverslips onto the imaging slide. Fluorescence and DIC images were acquired with an ORCA-Flash 4.0 camera (Hamamatsu) mounted on an Axio Imager.M2 fluorescence microscope with a 63x Plan-Apochromat objective (Carl Zeiss) and an HXP 120C light source with ZEN 2.6 software. Image processing was performed using OMERO.insight client (Allan et al., 2012), and analyzed with Fiji software (Schindelin et al., 2012).

To assess the recruitment of arrestin2 by CCR5, arrestin2-YFP- and CCR5-expressing cells were incubated with 1 µM chemokine ligands. Individual coverslips were removed and fixed with 4% PFA for 10 min at 0, 10, and 30 min post-ligand stimulation. Fixed cells were permeabilized with 0.1% Triton X-100 in PBS for 5 min, rinsed with PBS twice and blocked with 5% FBS in PBS. CCR5 was stained as mentioned previously and imaged. Colocalization between arrestin2 and CCR5 was assessed by measuring the Mander's coefficient in 2-3 regions of interest (ROI) of 100 µm$^2$ per cell using the Fiji JACOP plug-in (Bolte and Cordelières, 2006). The number of internalized CCR5 puncta with and without arrestin2 was quantified manually by taking 3 ROIs of 100 µm$^2$ per cell using Fiji.

To image arrestin2/CCR5 trafficking to lysosome, arrestin2-YFP and CCR5 expressing cells were treated with [6P4]CCL5. Individual coverslips were removed and fixed with 4% PFA for 10 min at 0, 10, and 30 min post stimulation. Fixed cells were permeabilized with 0.1% Triton X-100 in PBS for 5 min, rinsed with PBS twice and blocked with 5% FBS in PBS. Lysosomes were stained with LAMP1 antibody (1:200, Cell Signaling Technology, D2D11). CCR5 was stained with FLAG antibody (1:200, Thermo Fisher F3165). Secondary rabbit (1:500) Alexa-Fluor 568 (A110042 Invitrogen) and secondary mouse (1:500) Alexa-Fluor 633 (A21052, Invitrogen) fluorescent antibodies were used respectively. Fixation, imaging and analysis were performed as described above.

For assessing the effect of arrestin2 mutations, respective mutants were overexpressed with CCR5 in HeLa$^{-arr2/3}$ and HeLa cells, followed by immunostaining and microscopy analysis as described above (HeLa$^{-arr2/3}$: 60 min, HeLa: 30 min post [6P4]CCL5 stimulation).

## Live-cell imaging

For live-cell imaging, HeLa cells expressing arrestin2-YFP were seeded on an ibidi µ-slide VI 0.4 channel slide (#80606, Ibidi), 24 hours prior to data acquisition. Live cell imaging was performed in complete growth medium lacking phenol red at 37°C with 5% $CO_2$ 508 using an inverted Axio Observer microscope (Zeiss) with a Plan Apochromat N 63x/1.40 oil DIC 509 M27 objective and a Photometrics Prime 95B camera. Filters with standard specifications for GFP were used to image arrestin2-YFP. After selecting cells to be imaged, images were acquired at 5 min intervals. Image processing was performed using OMERO.insight client (Allan et al., 2012), and analyzed with Fiji software (Schindelin et al., 2012).

To image lysosome stained with lysotracker, HeLa cells expressing arrestin2-YFP and CCR5 were seeded on an ibidi µ-slide VI 0.4 channel slide (#80606, Ibidi), 24 hours prior to data acquisition. LysoTracker™ Deep Red (L12492) and peptide ligand was added in complete growth medium lacking phenol red. Images were taken at 0 min and 30 min.

## Statistics

Statistical analysis was performed using GraphPad Prism 10.1.1 (GraphPad Software, Inc., San Diego, CA, USA). For statistical evaluation, the normality of the data was routinely tested using the Shapiro-Wilk or Kolmogorov-Smirnov normality test. For the comparison of two groups (Figure 5A, B), a t-test was employed, whereas to compare three or more groups (Figure 4D), a one-way ANOVA was performed followed by a Kruskal-Wallis test.

## NMR Experiments

NMR samples were prepared in SEC buffer I supplemented with 5% $D_2O$, 2 mM EDTA and 0.03% $NaN_3$ as 270-µl volumes in Shigemi tubes. The assignment sample contained 300 mM NaCl. The spectra were recorded on a Bruker AVANCE 14.1 T (600 MHz) spectrometer (arrestin2$^{1\text{-}393}$, AP2β2$^{701\text{-}937}$) or a Bruker AVANCE 21.2 T (900 MHz) spectrometer (clathrin-N) equipped with a TCI cryoprobe at 303 K. The spectra were processed with NMRPipe (Delaglio et al., 1995), assigned using CcpNmr AnalysisAssign (Skinner et al., 2016), and analyzed with NMRFAM-SPARKY (Lee et al., 2015).

### Arrestin2 assignment

For the assignment of arrestin2 backbone resonances, HNCACB-TROSY, HNCA-TROSY and HNCO-TROSY spectra were recorded on $^{15}$N-, $^{13}$C-, $^{2}$H-labeled arrestin2$^{1\text{-}393}$ (100-150 µM) samples.

### Arrestin2 titrations

For detecting the clathrin-N-arrestin2 interaction on arrestin2 by NMR, a titration of 50 µM $^{15}$N-, $^{2}$H-labeled arrestin2$^{1\text{-}393}$ with unlabeled clathrin-N up to an equimolar amount was monitored by $^{1}$H-$^{15}$N HSQC-TROSY spectra recorded as 100 ($^{15}$N) x 512 ($^{1}$H) complex points and acquisition times of 50 ms ($^{15}$N) and 55 ms ($^{1}$H) for 4.5 h. Peak intensities $I$ were determined by integration and the interaction was quantified relative to the intensity $I_0$ in the absence of clathrin-N. An intensity attenuation larger than one standard deviation of $I/I_0$ calculated from all resonances was considered significant.

Similarly, a titration of 50 µM Ile-δ1-$^{13}CH_3$, $^{2}$H-labeled arrestin2$^{1\text{-}393}$ with unlabeled clathrin-N up to a concentration of 600 µM was monitored by $^{1}$H-$^{13}$C HMQC spectra recorded as 32 ($^{13}$C) x 512 ($^{1}$H) complex points and acquisition times of 20 ms ($^{13}$C) and 55 ms ($^{1}$H) for 1 h. The assignments of the methyl groups were transferred from BMRB ID:51131 (Shiraishi et al., 2021). $K_D$ values were obtained by nonlinear least-squares fitting using Matlab (Matlab_R2021b, MathWorks, Inc.) and the following equation:

$$\Delta\delta = \Delta\delta_{max}\frac{[L] + [P] + K_D - \sqrt{([L] + [P] + K_D)^2 - 4[P][L]}}{2[P]} \quad (1)$$

where $\Delta\delta = \delta_{apo}-\delta_{bound}$ is the difference in the $^{13}C$ chemical shift, $\delta_{max}$ is the difference between apo and the fully ligand-bound state, and [P] and [L] are the total protein (arrestin2) and ligand (clathrin-N) concentrations, respectively.

Combined $^{1}H/^{13}C$ chemical shift perturbations $\Delta\delta_{HC}$ were calculated from the relation:

$$\Delta\delta_{HC} = \sqrt{\Delta\delta_H{}^2 + \left(\frac{\Delta\delta_C}{3.6}\right)^2} \qquad (2)$$

where $\Delta\delta_H$ is the methyl proton and $\Delta\delta_C$ is the $^{13}C$-methyl chemical shift difference between the apo and bound state. $\Delta\delta_{HC}$ values greater than one standard deviation from the mean were considered significant.

### clathrin-N titrations

For detecting the clathrin-N-arrestin2 interaction on clathrin-N by NMR, a titration of 50 µM $^{15}N$-, $^{2}H$-labeled clathrin-N with unlabeled arrestin2$^{1-393}$, arrestin2$^{1-418}$, arrestin2$^{\Delta CBL}$ or arrestin2$^{1-393}$•CCR5pp6 up to an equimolar amount was monitored by $^{1}H$-$^{15}N$ HSQC-TROSY spectra recorded as 100 ($^{15}N$) x 1024 ($^{1}H$) complex points and acquisition times of 35 ms ($^{15}N$) and 80 ms ($^{1}H$) for 4.5 h. Assignments for clathrin-N were transferred from BMRB ID:25403 (Zhuo et al., 2015). Peak intensities were determined by quantifying peak volumes. Binding regions were determined by intensity ratios as described above.

### AP2β2 titrations

For detecting the AP2β2-arrestin2 interaction on AP2β2$^{701-937}$ by NMR, a titration of 50 µM $^{15}N$-, $^{2}H$-labeled AP2β2$^{701-937}$ with unlabeled arrestin2$^{1-418}$ or arrestin2$^{1-418}$•CCR5pp6 up to an equimolar amount was monitored by $^{1}H$-$^{15}N$ HSQC-TROSY spectra recorded as 100 ($^{15}N$) x 512 ($^{1}H$) complex points and acquisition times of 50 ms ($^{15}N$) and 55 ms ($^{1}H$) for 1 h. Assignments for AP2β2$^{701-937}$ were transferred from BMRB ID: 52320 (Naudi-Fabra et al., 2024). Peak intensities were determined by quantifying peak volumes. Binding regions were determined by intensity ratios as described above.

## SEC binding assay

SEC binding assays were performed on an UltiMate 3000 HPLC system. Samples containing single polypeptides or their mixtures as indicated in the text and figure legends (arrestin2$^{1-418}$: 10 µM, AP2β2: 10 µM, clathrin-N: 10 µM, CCR5pp0: 100 µM, CCR5pp3: 100 µM, CCR5pp4: 100 µM, CCR5pp6: 25-100 µM) were prepared as 270 µL volumes in SEC buffer II. Samples were injected with an autosampler using a 250-µL sample-loop onto a self-packed 4.2-ml S200 10/300 SEC column (length 25 mm, diameter 4.6 mm), which had been pre-equilibrated with SEC buffer II. Complex formation was monitored by following protein absorbance at 280 nm at 2.6 ml elution volume and the composition of the respective SEC fractions of all prepared complexes was analyzed by SDS-PAGE (Figure 3-figure supplement 2C).

The apparent dissociation constant of the arrestin2$^{1-418}$-AP2β2$^{701-937}$ complex in the presence of the CCR5 phosphopeptides could be determined by integrating the SEC absorption peaks of the complex and of the apo proteins and using their respective extinction coefficients. The increase of absorbance around 2.6 ml is a consequence of the additional AP2β2$^{701-937}$ in that elution region. This region overlaps to some extent with the elution profile of apo arrestin2$^{1-418}$.

Taking into account the 1:1 stoichiometry, the amount of formed complex was estimated by integrating the profile between 2.4 and 2.8 ml, subtracting the respective integral of the apo arrestin2$^{1-418}$ profile, and dividing the difference by the AP2β2$^{701-937}$ extinction coefficient. Since the phosphopeptides do not contain tryptophan, their absorbance contribution was ignored.

### Trypsin proteolysis

Trypsin proteolysis assays were carried out by pre-incubating 100 µL of 20 µM arrestin2$^{1-418}$ and 100 µM CCR5pp6 or 500 µM CCR5pp4/CCR5pp3 phosphopeptide with 1-(CCR5pp6), 2-(CCR5pp6) and 5-molar equivalents (CCR5pp6, CCR5pp4, CCR5pp3) of AP2β2 protein at room temperature for 5-10 min in the SEC buffer II. Following pre-incubation, 1 ng of Trypsin Gold (Promega) was added, and the mixture further incubated at 35 °C under gentle shaking (500 rpm, ThermoMixer). Samples for SDS-PAGE (10 µL mixed with 10 µL of 4x SDS loading buffer) were taken at 0, 5, 10, 20, 30, 60, and 90 min. The reaction was quenched by boiling the samples for 10 min at 95°C. Samples were then loaded on 4-20% precast gradient gels and visualized with Instant Blue protein stain (Abcam). Control reactions were run with apo arrestin2$^{1-418}$ and arrestin2$^{1-418}$ incubated with 100 µM CCR5pp6 or 60-500 µM CCR5pp4/CCR5pp3 phosphopeptide.

SDS-PAGE gels were analyzed using ImageJ software (Schneider et al., 2012) by integrating the peak area of the two bands corresponding to full-length arrestin2$^{1-418}$ (top) and arrestin2$^{1-418}$ cleaved at residue R393 (bottom). The relative abundance (in %) of arrestin2$^{1-418}$ was calculated from the respective integrals at 5 min upon trypsin addition.

## Data availability

All data needed to evaluate the conclusions in the paper are present in the main text and/or the Supplementary Information.

## Supplementary Information

| Phosphopeptide | Sequence | $K_D$ (arrestin2$^{1-393}$) [µM][a] |
|---|---|---|
| CCR5pp6 | APERASSVYTRSTGEQEISVGL | 45 ± 6 |
| CCR5pp4 | APERASSVYTRSTGEQEISVGL | 199 ± 10 |
| CCR5pp3 | APERASSVYTRSTGEQEISVGL | 198 ± 6 |

[a]data from Isaikina, Petrovic et al. (2023).

**Table S1. CCR5 phosphopeptide sequences and their affinities towards arrestin2.** Underlined serine or threonine residues are phosphorylated.

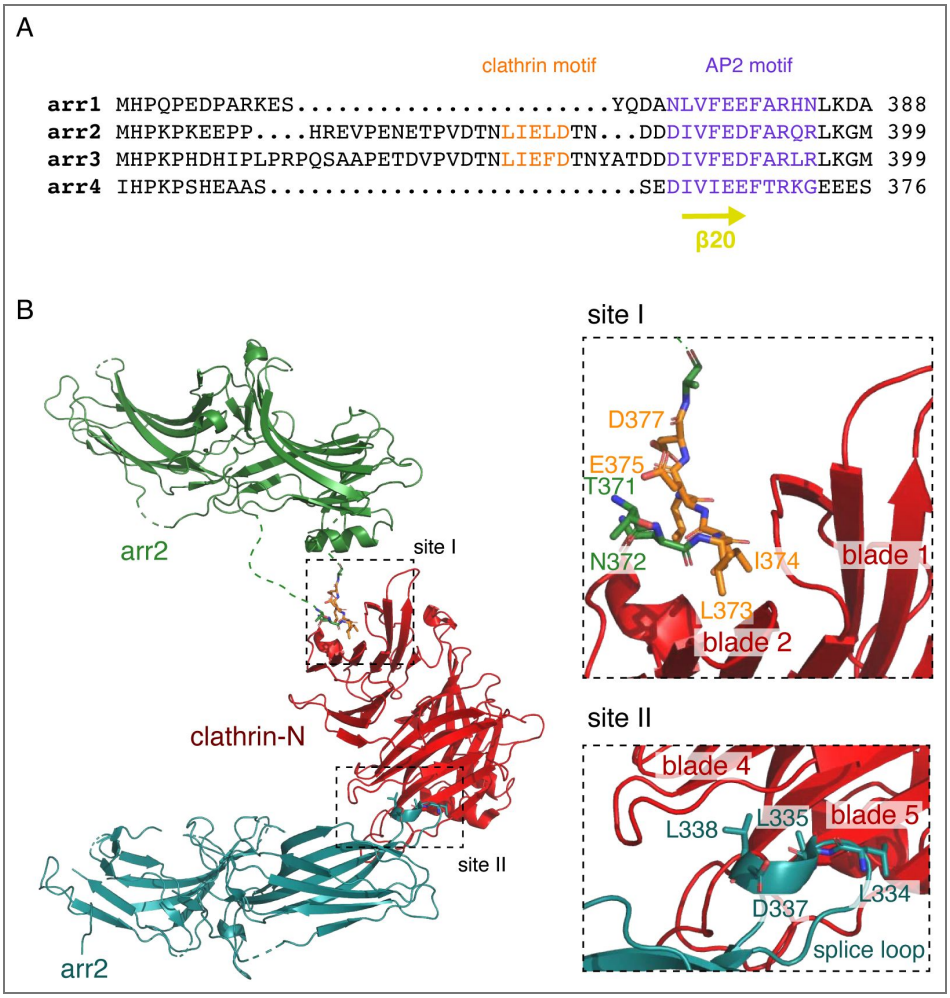


**Figure 1–figure supplement 1. Arrestin sequence alignment and analysis of the arrestin2-clathrin-N complex structure.**

(A) Sequence alignment of four human arrestin types. The clathrin-binding motif (orange) and AP2 binding motif (purple) are indicated within the sequences. The numbering on the right corresponds to the last amino acid in the alignment. (B) X-ray structure of the arrestin2-clathrin complex (PDB:3GD1[45]). The structure shows two arrestin chains (green and blue) interacting with one clathrin-N molecule (red). Interaction sites 1 and 2 are indicated by dashed rectangles with enlarged views on the right. The arrestin2 residues involved in the interaction are shown as sticks. Site I: between CBL of arrestin2 (green) and the edge of β-sheet blade 1 and 2 of clathrin-N. CBL residues are shown as sticks. The numbering follows the PDB deposition. Site II: between arrestin2 splice loop (blue) and β-sheet blade 4 and 5 of clathrin-N.

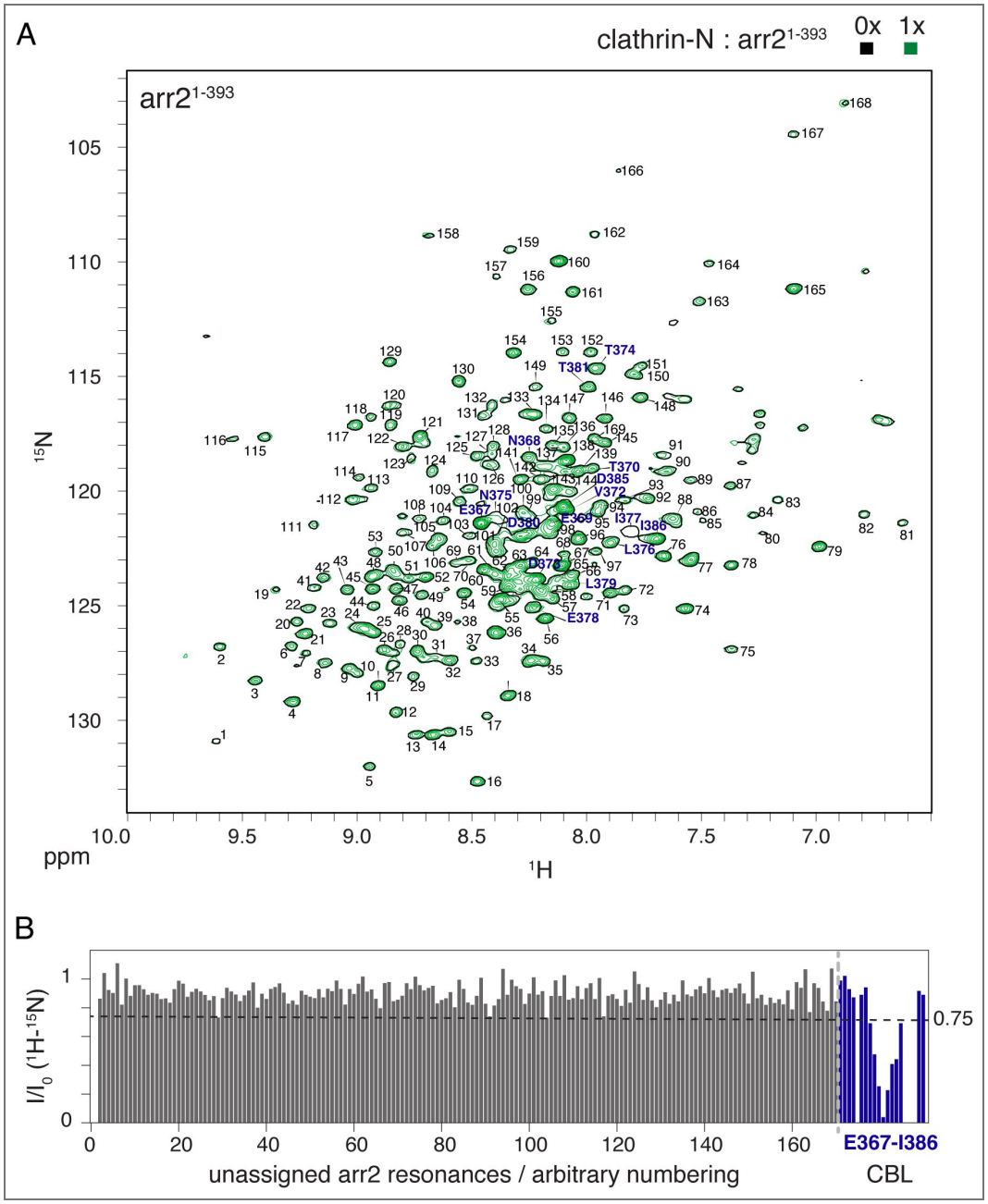


**Figure 1–figure supplement 2. Mapping of clathrin-N interaction on arrestin2.**

(A) $^{1}H$-$^{15}N$ TROSY spectrum of arrestin2$^{1-393}$ in apo (black) or upon equimolar addition of clathrin-N (green) recorded on a Bruker AVANCE 14.1 T (600 MHz) spectrometer equipped with a TCI cryoprobe at 303 K. Assigned resonances are marked by blue amino acid numbers. Unassigned resonances are marked by black arbitrary numbers. (B) Intensity reduction $I/I_0$ of arrestin2$^{1-393}$ $^{1}H$-$^{15}N$ TROSY resonances upon clathrin-N interaction. The dashed line is drawn at one standard deviation below the average $I/I_0$ value. The resonance numbering follows panel (A).

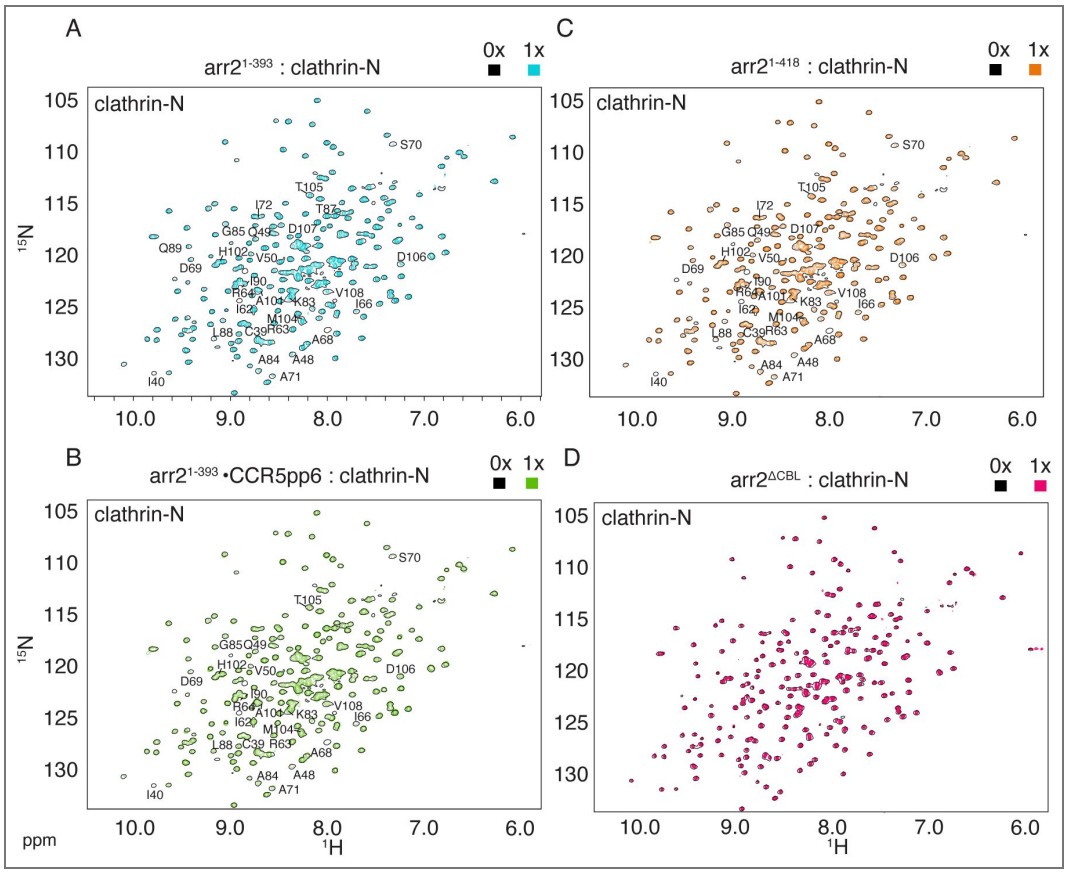


**Figure 2–figure supplement 1. Mapping of arrestin2 interaction on clathrin-N.**

$^{1}$H-$^{15}$N TROSY spectra of clathrin-N in the presence of one molar equivalent of (A) arrestin2$^{1-393}$ (cyan); (B) arrestin2$^{1-393}$•CCR5pp6 (green); (C) arrestin2$^{1-418}$ (orange) or (D), arrestin2 $^{\Delta CBL}$ (red) superimposed on $^{1}$H-$^{15}$N TROSY spectrum of apo clathrin-N (black). The spectra were recorded on a Bruker AVANCE 21.1 T (900 MHz) spectrometer equipped with a TCI cryoprobe at 303 K. Assigned residues undergoing significant line broadening are indicated on the spectra.

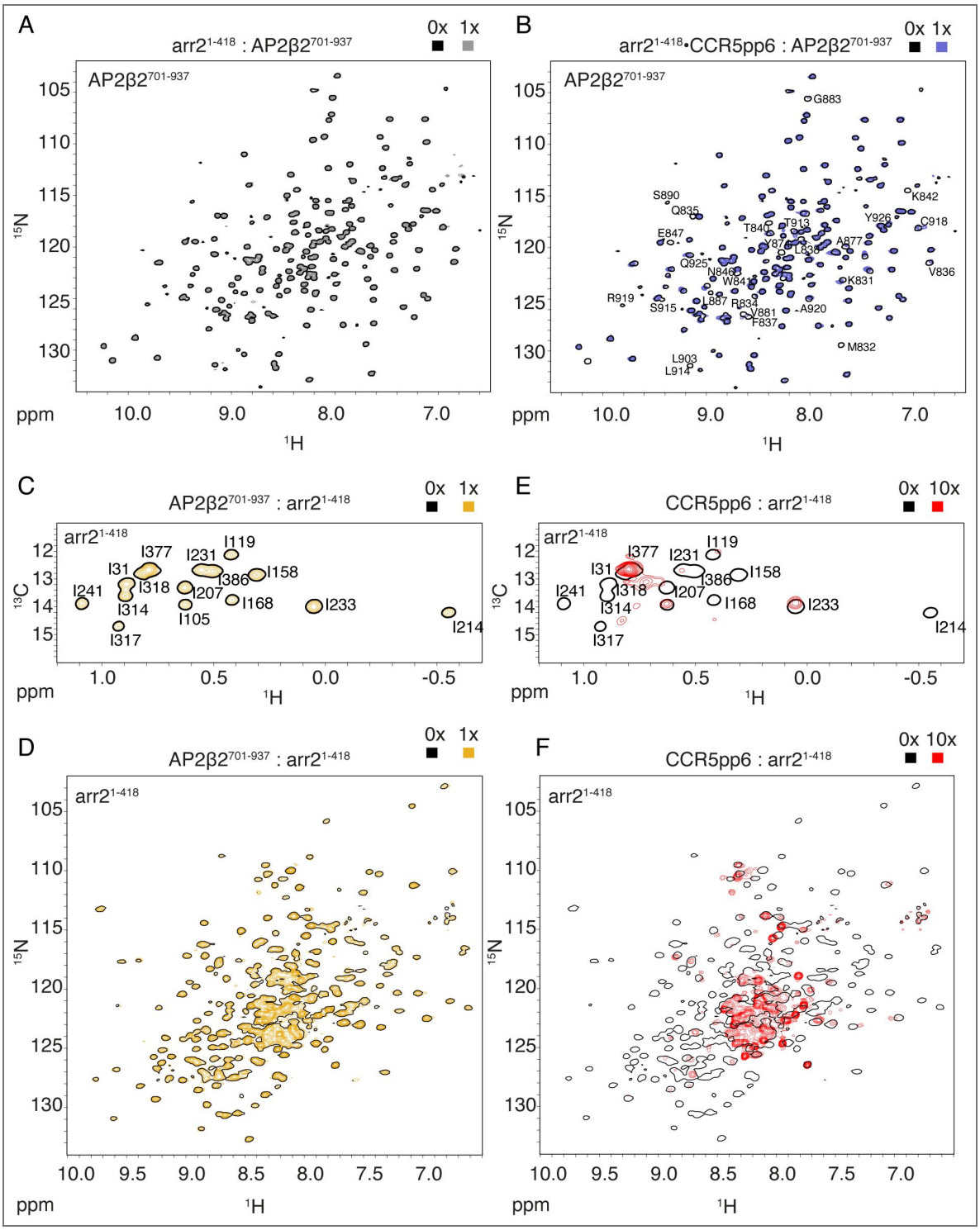


**Figure 3 – figure supplement 1. Arrestin2 interaction with the C-terminal domain of AP2β2 detected by NMR.**

(A, B) $^{1}$H-$^{15}$N TROSY spectra of AP2β2$^{701-937}$ in the absence or presence of one molar equivalent of either arrestin2$^{1-418}$ (A) or arrestin2$^{1-418}$•CCR5pp6 (B). Assigned residues undergoing significant intensity reduction are indicated on the spectra. (C, D) Test of interaction of arrestin2$^{1-418}$ with AP2β2$^{701-937}$. (C) $^{1}$H-$^{13}$C HMQC (Ile-δ1-$^{13}CH_3$, $^{2}$H-labeled arrestin2$^{1-418}$) and (D) $^{1}$H-$^{15}$N TROSY ($^{15}$N, $^{2}$H-labeled arrestin2$^{1-418}$) spectra of arrestin2$^{1-418}$ in the absence or presence of one molar equivalent of AP2β2$^{701-937}$. (E, F) Test of interaction of arrestin2$^{1-418}$ with CCR5pp6. (E) $^{1}$H-$^{13}$C HMQC (Ile-δ1-$^{13}CH_3$, $^{2}$H-labeled arrestin2$^{1-418}$) and (F) $^{1}$H-$^{15}$N TROSY ($^{15}$N, $^{2}$H-labeled arrestin2$^{1-418}$) spectra of arrestin2$^{1-418}$ in the absence or presence of a ten-molar equivalent of CCR5pp6.

**Figure 3–figure supplement 2. Arrestin2 interaction with clathrin-N and AP2β2 monitored by SEC.**

(A) SEC profiles of arrestin2$^{1-418}$, clathrin-N and their mixture. (B) as in (A) but in the presence of AP2β2$^{701-937}$ and CCR5pp6. (C) SDS-PAGE of sample from the SEC complex fraction (taken at 2.6ml) monitoring the formation of the arrestin2/AP2β2 complex for various conditions indicated on the top. The empty square indicates the expected position of clathrin-N.

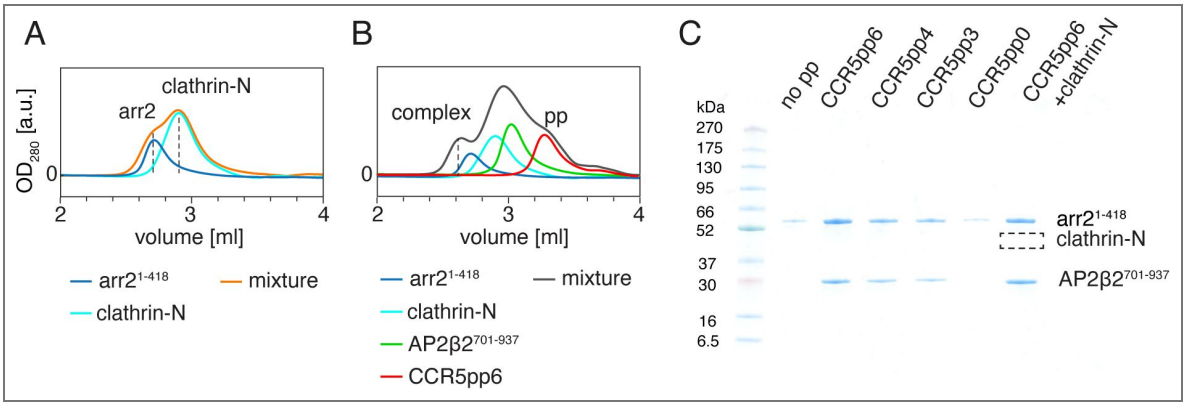


**Figure 3–figure supplement 3. Arrestin2$^{1-418}$ trypsin proteolysis assay.**

Trypsin proteolysis of arrestin2$^{1-418}$ in apo form and in complexes with (A) CCR5pp6, (B) CCR5pp3 and (C) CCR5pp4 and AP2β2$^{701-937}$ detected by SDS-PAGE. The incubation time is indicated on the top. 'M' indicates the protein size marker. The table on the right indicates sample composition and the relative abundance of arrestin2$^{1-418}$ after 5 min. incubation (see Materials and Methods). The activation by the CCR5 phosphopeptides accelerates arrestin2$^{1-418}$ proteolysis. The addition of AP2β2$^{701-937}$ reverses this effect.

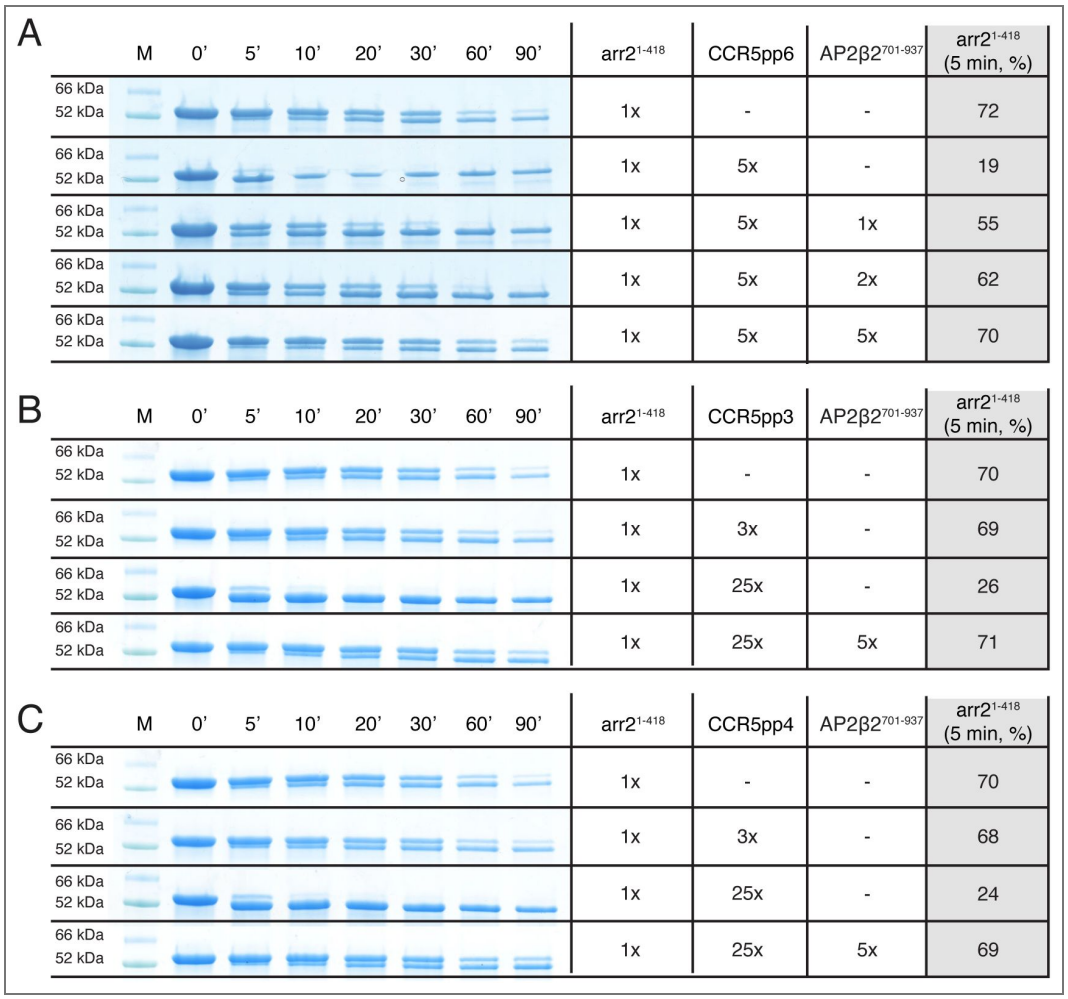


| arr2$^{1-418}$ | CCR5pp6 | AP2β2$^{701-937}$ | arr2$^{1-418}$ (5 min, %) |
|---|---|---|---|
| 1x | - | - | 72 |
| 1x | 5x | - | 19 |
| 1x | 5x | 1x | 55 |
| 1x | 5x | 2x | 62 |
| 1x | 5x | 5x | 70 |




| arr2$^{1-418}$ | CCR5pp3 | AP2β2$^{701-937}$ | arr2$^{1-418}$ (5 min, %) |
|---|---|---|---|
| 1x | - | - | 70 |
| 1x | 3x | - | 69 |
| 1x | 25x | - | 26 |
| 1x | 25x | 5x | 71 |




| arr2$^{1-418}$ | CCR5pp4 | AP2β2$^{701-937}$ | arr2$^{1-418}$ (5 min, %) |
|---|---|---|---|
| 1x | - | - | 70 |
| 1x | 3x | - | 68 |
| 1x | 25x | - | 24 |
| 1x | 25x | 5x | 69 |

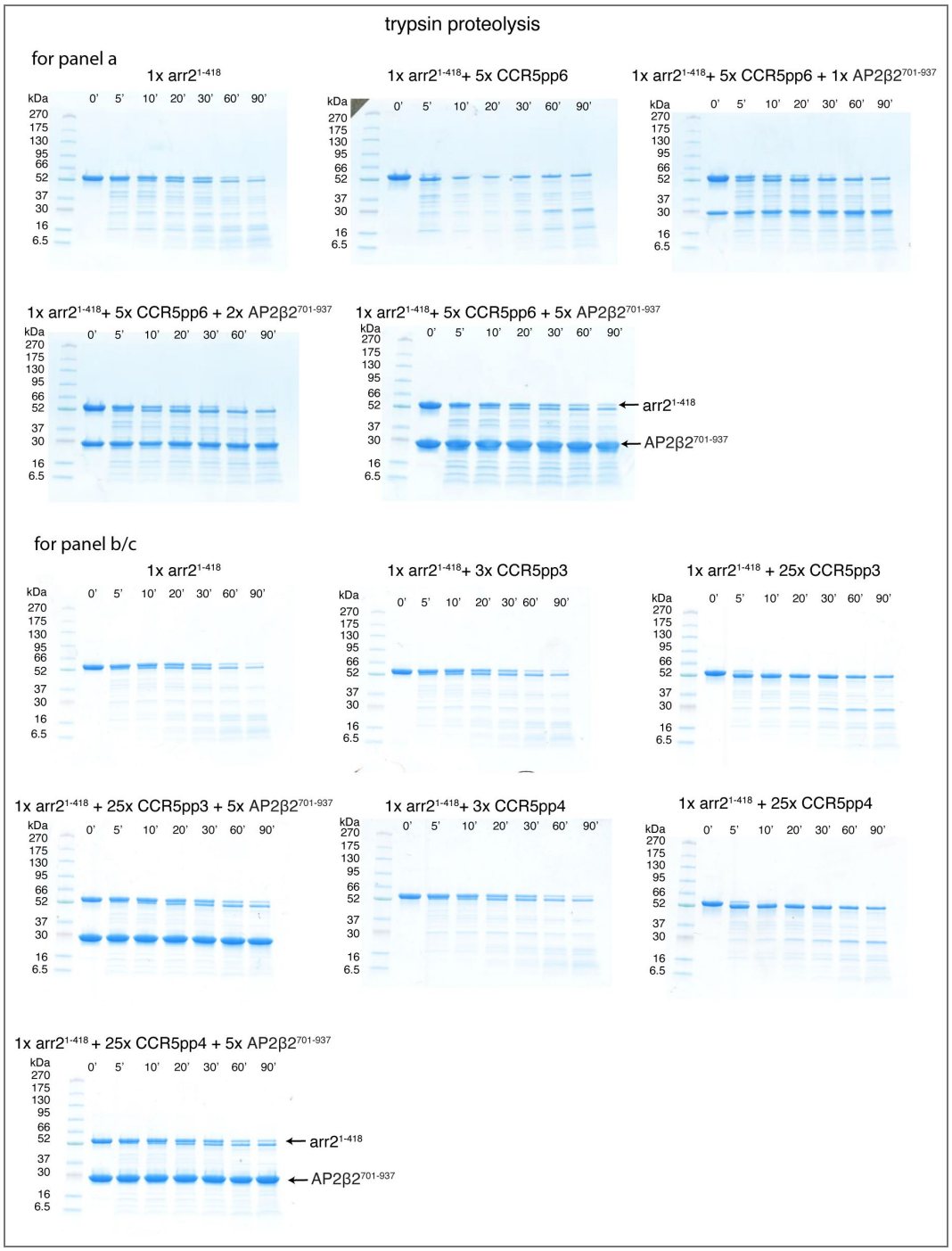


**Figure 3–figure supplement 4. Uncropped SDS-PAGE gels of the arrestin2$^{1-418}$ trypsin proteolysis.**

SDS-PAGE gels for the data in Figure 3–figure supplement 3. The composition of the sample and the reaction incubation time are indicated at the top. Protein marker bands are indicated on the left. Arrestin2$^{1-418}$ runs at ~ 52 kDa, AP2β2$^{701-937}$ at ~ 30 kDa.

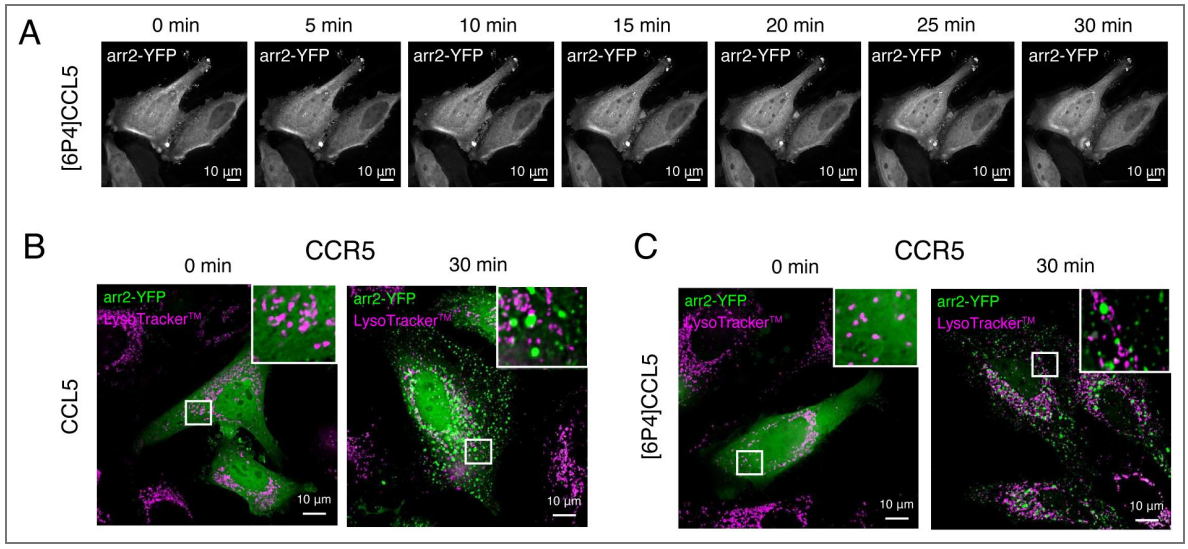


**Figure 4–figure supplement 1. Arrestin2 internalization (control) and re-localization in live HeLa cells upon chemokine stimulation in the presence of CCR5.**

(A) HeLa cells transfected only with arrestin2-YFP and stimulated with 6P4[CCL5]. In the absence of the receptor, arrestin2 stays distributed in the cell cytoplasm and nucleus. (B,C) Arrestin2-YFP re-localization in HeLa cells transfected with wild-type CCR5 and arrestin2-YFP genes. Arrestin2-YFP and LysoTrackerTM signals were used to monitor the protein trafficking for up to 30 min after CCL5 (B) or 6P4[CCL5] (C) incubation. No overlap between the LysoTrackerTM and arrestin2 signal has been detected. White squares indicate zoomed regions of interest.

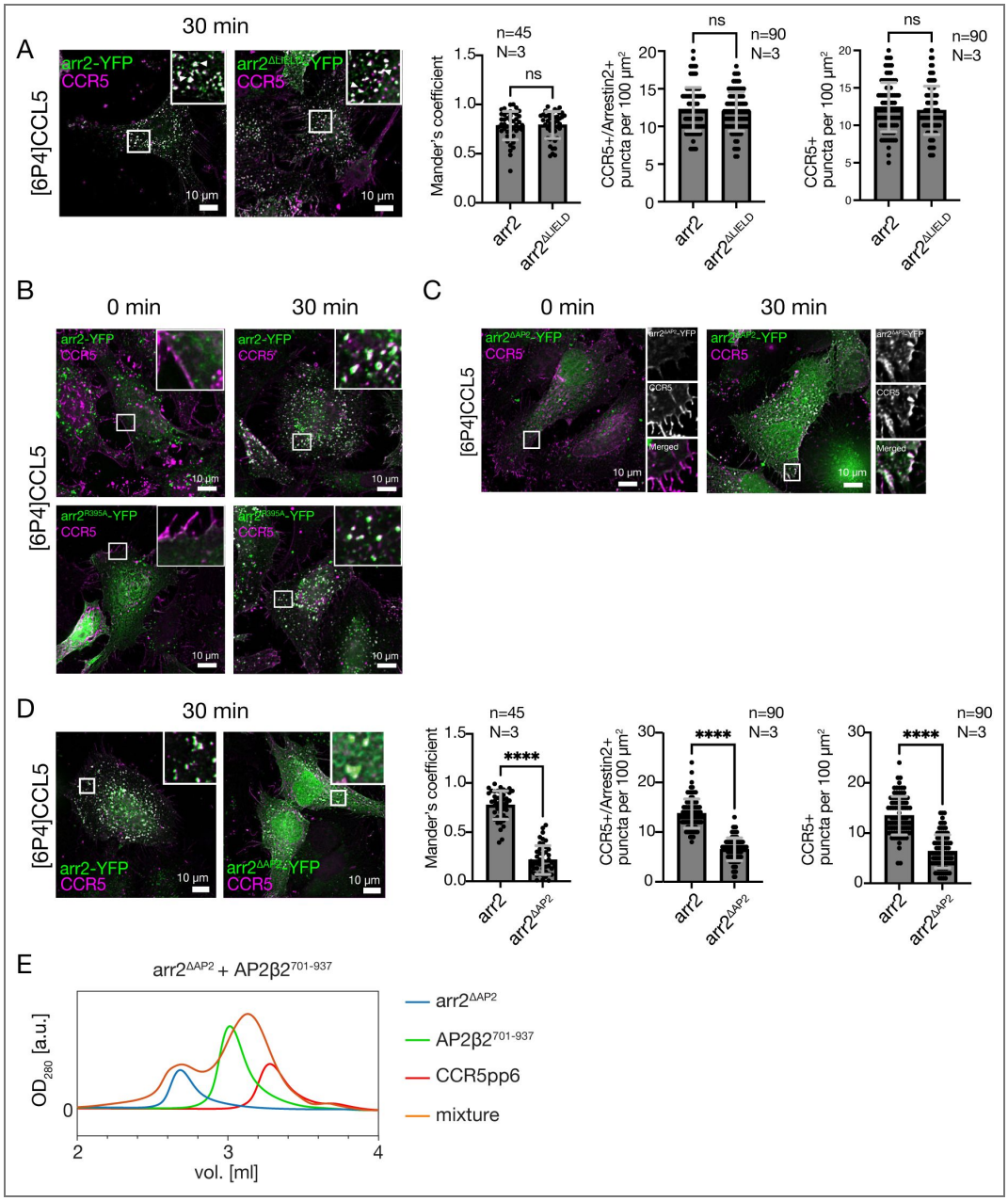


**Figure 5–figure supplement 1. Dependence of CCR5 internalization on the interactions of arrestin2 with clathrin or AP2 monitored in HeLa (CCL2) cells by immunofluorescence microscopy.**

(A) CCR5 internalization induced by [6P4]CCL5 in HeLa cells co-transfected with plasmids containing either arrestin2-YFP or arrestin2$^{\Delta LIELD}$-YFP, which misses the clathrin-binding motif. No significant difference is detected as quantified by the Mander's colocalization coefficient (ns, not significant: P > 0.9999) or by counting CCR5$^{+}$/Arrestin2$^{+}$ and only CCR5$^{+}$ puncta 30 min after ligand incubation. Mean and standard deviation are shown for N=3 biological replicates and n=45 ROI from 20 cells (Mander's) or n=90 ROI from 30 cells (puncta counting). (B) CCR5 internalization induced by 6P4[CCL5] in HeLa cells co-transfected with plasmids containing either arrestin2-YFP or arrestin2$^{R395A}$-YFP, which bears a single mutation in the adaptin-binding motif. The mutation does not affect CCR5 internalization up to 30 min after 6P4[CCL5] stimulation. (C) Recruitment of arrestin2 $^{\Delta AP2}$-YFP to CCR5 in the HeLa cell plasma membrane upon [6P4]CCL5 ligand stimulation. (D) CCR5 internalization induced by [6P4]CCL5 in HeLa cells co-transfected with plasmids containing either arrestin2-YFP or arrestin2$^{\Delta AP2}$-YFP. Mean and standard deviation of the Mander's coefficient and the number of puncta were determined as in (A). The absence of the AP2 binding motif in the arrestin2$^{\Delta AP2}$-YFP construct causes a significant (****: P < 0.0001) reduction of CCR5 internalization 30 min after ligand incubation. (E) SEC profiles of arrestin2$^{\Delta AP2}$, AP2β2$^{701-937}$, CCR5pp6 and their mixture. No complex formation is observed.

# Acknowledgements

We gratefully acknowledge I. Hertel and M. Rogowski for the expression and purification of proteases and CCL5 ligands. We thank Prof. Mariagrazia Uguccioni and Dr. Valentina Cecchinato (Institute for Research in Biomedicine, Bellinzona, Switzerland) for the HeLa$^{-arr2/3}$ cells and Prof. Arun Shukla for helpful discussions. This work was supported by the Swiss National Science Foundation (grants 31-201270 and IZLIZ3-200298 to S.G., 31-197779 and 31-185127 to A.S.), and by a Fellowship for Excellence by the Biozentrum Basel International PhD Program to I.P.


# Additional information

## Author contributions

I.P., S.D., P.I., A.S., and S.G. conceived the study. I.P. and L.A.A generated all the constructs and mutants for the cellular assays. S.D. performed the cellular assays and analyzed the cellular data with guidance from A.S. I.P. expressed and purified proteins. I.P. recorded NMR experiments and analyzed NMR data. I.P. designed and analyzed SEC and trypsin proteolysis assay. I.P. and S.G. wrote the manuscript with inputs from all co-authors.


## Funding

| Funder | Grant reference number | Author |
|---|---|---|
| Schweizerischer Nationalfonds zur Förderung der Wissenschaftlichen Forschung (SNF) | IZLIZ3-200298 | Stephan Grzesiek |
| Schweizerischer Nationalfonds zur Förderung der Wissenschaftlichen Forschung (SNF) | 31-19777 | Anne Spang |
| Schweizerischer Nationalfonds zur Förderung der Wissenschaftlichen Forschung (SNF) | 31-185127 | Anne Spang |



## Author ORCID iDs

**Ivana Petrovic**: https://orcid.org/0000-0003-4461-7603
**Samit Desai**: https://orcid.org/0009-0002-4175-6659
**Polina Isaikina**: https://orcid.org/0000-0003-4466-7715
**Layara Akemi Abiko**: https://orcid.org/0000-0003-3537-534X
**Anne Spang**: https://orcid.org/0000-0002-2387-6203
**Stephan Grzesiek**: https://orcid.org/0000-0003-1998-4225


# References


**Alkhatib G** (2009) The biology of CCR5 and CXCR4. *Current Opinion in HIV and AIDS* **4**:96-103 https://doi.org/10.1097/COH.0b013e328324bbec

**Allan C,** Burel J-M, Moore J, Blackburn C, Linkert M, Loynton S, MacDonald D, Moore WJ, Neves C, Patterson A, *et al.* (2012) OMERO: flexible, model-driven data management for experimental biology. *Nat Methods* **9**:245-253 https://doi.org/10.1038/nmeth.1896

**Ariel A,** Fredman G, Sun Y-P, Kantarci A, Van Dyke TE, Luster AD, Serhan CN. (2006) Apoptotic neutrophils and T cells sequester chemokines during immune response resolution through modulation of CCR5 expression. *Nat Immunol* **7**:1209-1216 https://doi.org/10.1038/ni1392

**Barsi-Rhyne B,** Manglik A, von Zastrow M. (2022) Discrete GPCR-triggered endocytic modes enable β-arrestins to flexibly regulate cell signaling. *eLife* **11**:e81563 https://doi.org/10.7554/eLife.81563

**Beautrait A,** Paradis JS, Zimmerman B, Giubilaro J, Nikolajev L, Armando S, Kobayashi H, Yamani L, Namkung Y, Heydenreich FM, *et al.* (2017) A new inhibitor of the β-arrestin/AP2 endocytic complex reveals interplay between GPCR internalization and signalling. *Nat Commun* **8**:15054 https://doi.org/10.1038/ncomms15054

**Benz C,** Ali M, Krystkowiak I, Simonetti L, Sayadi A, Mihalic F, Kliche J, Andersson E, Jemth P, Davey NE, *et al.* (2022) Proteome-scale mapping of binding sites in the unstructured regions of the human proteome. *Molecular Systems Biology* **18**:e10584 https://doi.org/10.15252/msb.202110584

**Bolte S,** Cordelières FP (2006) A guided tour into subcellular colocalization analysis in light microscopy. *Journal of Microscopy* **224**:213-232 https://doi.org/10.1111/j.1365-2818.2006.01706.x

**Bous J,** Fouillen A, Orcel H, Trapani S, Cong X, Fontanel S, Saint-Paul J, Lai-Kee-Him J, Urbach S, Sibille N, *et al.* (2022) Structure of the vasopressin hormone-V2 receptor-β-arrestin1 ternary complex. *Sci Adv* **8**:eabo7761 https://doi.org/10.1126/sciadv.abo7761

**Collins BM,** McCoy AJ, Kent HM, Evans PR, Owen DJ (2002) Molecular Architecture and Functional Model of the Endocytic AP2 Complex. *Cell* **109**:523-535 https://doi.org/10.1016/S0092-8674(02)00735-3

**Congreve M,** de Graaf C, Swain NA, Tate CG. (2020) Impact of GPCR Structures on Drug Discovery. *Cell* **181**:81-91 https://doi.org/10.1016/j.cell.2020.03.003

**D'Agostino G,** Artinger M, Locati M, Perez L, Legler DF, Bianchi ME, Rüegg C, Thelen M, Marchese A, Rocchi MBL, *et al.* (2020) β-Arrestin1 and β-Arrestin2 Are Required to Support the Activity of the CXCL12/HMGB1 Heterocomplex on CXCR4. *Front Immunol* **11**:550824 https://doi.org/10.3389/fimmu.2020.550824

**Delaglio F,** Grzesiek S, Vuister GW, Zhu G, Pfeifer J, Bax A (1995) NMRPipe: A multidimensional spectral processing system based on UNIX pipes. *J Biomol NMR* **6**:277-293 https://doi.org/10.1007/BF00197809

**Dell'Angelica EC** (2001) Clathrin-binding proteins: Got a motif?. *Join the network! Trends in Cell Biology* **11**:315-318 https://doi.org/10.1016/S0962-8924(01)02043-8

**Escola J-M,** Kuenzi G, Gaertner H, Foti M, Hartley O (2010) CC Chemokine Receptor 5 (CCR5) Desensitization: CYCLING RECEPTORS ACCUMULATE IN THE TRANS-GOLGI NETWORK*. *Journal of Biological Chemistry* **285**:41772-41780 https://doi.org/10.1074/jbc.M110.153460

**Fraile-Ramos A,** Kohout TA, Waldhoer M, Marsh M (2003) Endocytosis of the Viral Chemokine Receptor US28 Does Not Require Beta-Arrestins But Is Dependent on the Clathrin-Mediated Pathway. *Traffic* **4**:243-253 https://doi.org/10.1034/j.1600-0854.2003.00079.x

**Gaertner H,** Cerini F, Escola J-M, Kuenzi G, Melotti A, Offord R, Rossitto-Borlat I, Nedellec R, Salkowitz J, Gorochov G, *et al.* (2008) Highly potent, fully recombinant anti-HIV chemokines: Reengineering a low-cost microbicide. *PNAS* **105**:17706-17711 https://doi.org/10.1073/pnas.0805098105

**Goodman OB,** Krupnick JG, Gurevich VV, Benovic JL, Keen JH (1997) Arrestin/Clathrin Interaction: Localization of the arrestin binding locus to the clathrin terminal domain. *Journal of Biological Chemistry* **272**:15017-15022 https://doi.org/10.1074/jbc.272.23.15017

**Goodman OB,** Krupnick JG, Santini F, Gurevich VV, Penn RB, Gagnon AW, Keen JH, Benovic JL (1996) β-Arrestin acts as a clathrin adaptor in endocytosis of the β2-adrenergic receptor. *Nature* **383**:447-450 https://doi.org/10.1038/383447a0

**Gu S,** Maurya S, Lona A, Borrega-Roman L, Salanga C, Gonzalez DJ, Kufareva I, Handel TM (2023) Ligand-Dependent Mechanisms of C-C Chemokine Receptor 5 (CCR5) Trafficking Revealed by APEX2 Proximity Labeling Proteomics. *bioRxiv* 2023.11.01.565224 https://doi.org/10.1101/2023.11.01.565224

**Gurevich VV,** Gurevich EV (2019) GPCR Signaling Regulation: The Role of GRKs and Arrestins. *Frontiers in Pharmacology* **10**

**Han M,** Gurevich VV, Vishnivetskiy SA, Sigler PB, Schubert C (2001) Crystal Structure of β-Arrestin at 1.9 Å: Possible Mechanism of Receptor Binding and Membrane Translocation. *Structure* **9**:869-880 https://doi.org/10.1016/S0969-2126(01)00644-X

**Hanyaloglu AC,** Zastrow M von (2008) Regulation of GPCRs by Endocytic Membrane Trafficking and Its Potential Implications. *Annu Rev Pharmacol Toxicol* **48**:537-568 https://doi.org/10.1146/annurev.pharmtox.48.113006.094830

**Huang W,** Masureel M, Qu Q, Janetzko J, Inoue A, Kato HE, Robertson MJ, Nguyen KC, Glenn JS, Skiniotis G, *et al.* (2020) Structure of the neurotensin receptor 1 in complex with β-arrestin 1. *Nature* **579**:303-308 https://doi.org/10.1038/s41586-020-1953-1

**Hughes CE,** Nibbs RJB (2018) A guide to chemokines and their receptors. *The FEBS Journal* **285**:2944-2971 https://doi.org/10.1111/febs.14466

**Isaikina P,** Petrovic I, Jakob RP, Sarma P, Ranjan A, Baruah M, Panwalkar V, Maier T, Shukla AK, Grzesiek S (2023) A key GPCR phosphorylation motif discovered in arrestin2·CCR5 phosphopeptide complexes. *Molecular Cell* **83**:2108-2121.e7. https://doi.org/10.1016/j.molcel.2023.05.002

**Isaikina P,** Tsai C-J, Dietz N, Pamula F, Grahl A, Goldie KN, Guixà-González R, Branco C, Paolini-Bertrand M, Calo N, *et al.* (2021) Structural basis of the activation of the CC chemokine receptor 5 by a chemokine agonist. *Science Advances* https://doi.org/10.1126/sciadv.abg8685

**Isaikina P,** Tsai C-J, Petrovic I, Rogowski M, Dürr AM, Grzesiek S (2022) Chapter 6 - Preparation of a stable CCL5·CCR5·Gi signaling complex for Cryo-EM analysis In: Shukla AK, editor. Methods in Cell Biology. *Biomolecular Interactions Part B* 115-141 https://doi.org/10.1016/bs.mcb.2022.03.001

**Jackson LP,** Kelly BT, McCoy AJ, Gaffry T, James LC, Collins BM, Höning S, Evans PR, Owen DJ (2010) A Large-Scale Conformational Change Couples Membrane Recruitment to Cargo Binding in the AP2 Clathrin Adaptor Complex. *Cell* **141**:1220-1229 https://doi.org/10.1016/j.cell.2010.05.006

**Janetzko J,** Kise R, Barsi-Rhyne B, Siepe DH, Heydenreich FM, Kawakami K, Masureel M, Maeda S, Garcia KC, Von Zastrow M, *et al.* (2022) Membrane phosphoinositides regulate GPCR-β-arrestin complex assembly and dynamics. *Cell* **185**:4560-4573.e19. https://doi.org/10.1016/j.cell.2022.10.018

**Jean-Charles P-Y,** Kaur S, Shenoy SK (2017) G Protein–Coupled Receptor Signaling Through β-Arrestin–Dependent Mechanisms. *Journal of Cardiovascular Pharmacology* **70**:142 https://doi.org/10.1097/FJC.0000000000000482

**Jiao X,** Nawab O, Patel T, Kossenkov AV, Halama N, Jaeger D, Pestell RG (2019) Recent Advances Targeting CCR5 for Cancer and Its Role in Immuno-Oncology. *Cancer Res* **79**:4801-4807 https://doi.org/10.1158/0008-5472.CAN-19-1167

**Jumper J,** Evans R, Pritzel A, Green T, Figurnov M, Ronneberger O, Tunyasuvunakool K, Bates R, Žídek A, Potapenko A, *et al.* (2021) Highly accurate protein structure prediction with AlphaFold. *Nature* **596**:583-589 https://doi.org/10.1038/s41586-021-03819-2

**Kaksonen M,** Roux A (2018) Mechanisms of clathrin-mediated endocytosis. *Nat Rev Mol Cell Biol* **19**:313-326 https://doi.org/10.1038/nrm.2017.132

**Kang DS,** Kern RC, Puthenveedu MA, von Zastrow M, Williams JC, Benovic JL. (2009) Structure of an Arrestin2-Clathrin Complex Reveals a Novel Clathrin Binding Domain That Modulates Receptor Trafficking. *J Biol Chem* **284**:29860-29872 https://doi.org/10.1074/jbc.M109.023366

**Kang Y,** Zhou XE, Gao X, He Y, Liu W, Ishchenko A, Barty A, White TA, Yefanov O, Han GW, *et al.* (2015) Crystal structure of rhodopsin bound to arrestin by femtosecond X-ray laser. *Nature* **523**:561-567 https://doi.org/10.1038/nature14656

**Kelly BT,** Graham SC, Liska N, Dannhauser PN, Höning S, Ungewickell EJ, Owen DJ (2014) AP2 controls clathrin polymerization with a membrane-activated switch. *Science* **345**:459-463 https://doi.org/10.1126/science.1254836

**Kern RC,** Kang DS, Benovic JL (2009) Arrestin2/Clathrin Interaction Is Regulated by Key N- and C-Terminal Regions in Arrestin2. *Biochemistry* **48**:7190-7200 https://doi.org/10.1021/bi900369c

**Kim Y-M,** Benovic JL (2002) Differential Roles of Arrestin-2 Interaction with Clathrin and Adaptor Protein 2 in G Protein-coupled Receptor Trafficking. *Journal of Biological Chemistry* **277**:30760-30768 https://doi.org/10.1074/jbc.M204528200

**Komolov KE,** Benovic JL (2018) G protein-coupled receptor kinases: Past, present and future. *Cellular Signalling*. *Honor of Bob Lefkowitz* **41**:17-24 https://doi.org/10.1016/j.cellsig.2017.07.004

**Kovtun O,** Dickson VK, Kelly BT, Owen DJ, Briggs JAG (2020) Architecture of the AP2/clathrin coat on the membranes of clathrin-coated vesicles. *Science Advances* **6**:eaba8381. https://doi.org/10.1126/sciadv.aba8381

**Krupnick JG,** Goodman OB, Keen JH, Benovic JL (1997) Arrestin/Clathrin Interaction: Localization of the clathrin binding domain of nonvisual arrestins to the carboxyl terminus. *Journal of Biological Chemistry* **272**:15011-15016 https://doi.org/10.1074/jbc.272.23.15011

**Lally CCM,** Bauer B, Selent J, Sommer ME (2017) C-edge loops of arrestin function as a membrane anchor. *Nat Commun* **8**:14258 https://doi.org/10.1038/ncomms14258

**Laporte SA,** Miller WE, Kim K-M, Caron MG (2002) β-Arrestin/AP-2 Interaction in G Protein-coupled Receptor Internalization: Identification of a β-arrestin binding site in β2-adaptin. *Journal of Biological Chemistry* **277**:9247-9254 https://doi.org/10.1074/jbc.M108490200

**Laporte SA,** Oakley RH, Holt JA, Barak LS, Caron MG (2000) The Interaction of β-Arrestin with the AP-2 Adaptor Is Required for the Clustering of β2-Adrenergic Receptor into Clathrin-coated Pits*. *Journal of Biological Chemistry* **275**:23120-23126 https://doi.org/10.1074/jbc.M002581200

**Lee W,** Tonelli M, Markley JL (2015) NMRFAM-SPARKY: enhanced software for biomolecular NMR spectroscopy. *Bioinformatics* **31**:1325-1327 https://doi.org/10.1093/bioinformatics/btu830

**Lemmon SK,** Traub LM (2012) Getting in Touch with the Clathrin Terminal Domain. *Traffic* **13**:511-519 https://doi.org/10.1111/j.1600-0854.2011.01321.x

**Maharana J,** Sarma P, Yadav MK, Sayantan Saha, Singh V, Shirsha Saha, Chami M, Banerjee R, Shukla AK (2023) Structural snapshots uncover a key phosphorylation motif in GPCRs driving β-arrestin activation. *Molecular Cell* **83**:2091-2107.e7. https://doi.org/10.1016/j.molcel.2023.04.025

**Martins E,** Brodier H, Rossitto-Borlat I, Ilgaz I, Villard M, Hartley O (2020) Arrestin Recruitment to C-C Chemokine Receptor 5: Potent C-C Chemokine Ligand 5 Analogs Reveal Differences in Dependence on Receptor Phosphorylation and Isoform-Specific Recruitment Bias. *Mol Pharmacol* **98**:599-611 https://doi.org/10.1124/molpharm.120.000036

**Moaven H,** Koike Y, Jao CC, Gurevich VV, Langen R, Chen J (2013) Visual arrestin interaction with clathrin adaptor AP-2 regulates photoreceptor survival in the vertebrate retina. *Proceedings of the National Academy of Sciences* **110**:9463-9468 https://doi.org/10.1073/pnas.1301126110

**Moo EV,** Senten JR van, Bräuner-Osborne H, Møller TC. (2021) Arrestin-Dependent and -Independent Internalization of G Protein–Coupled Receptors: Methods, Mechanisms, and Implications on Cell Signaling. *Mol Pharmacol* **99**:242-255 https://doi.org/10.1124/molpharm.120.000192

**Mueller A,** Kelly E, Strange PG (2002) Pathways for internalization and recycling of the chemokine receptor CCR5. *Blood* **99**:785-791 https://doi.org/10.1182/blood.V99.3.785

**Naudi-Fabra S,** Elena-Real CA, Vedel IM, Tengo M, Motzny K, Jiang P-L, Schmieder P, Liu F, Milles S (2024) An extended interaction site determines binding between AP180 and AP2 in clathrin mediated endocytosis. *Nat Commun* **15**:5884 https://doi.org/10.1038/s41467-024-50212-4

**Oakley RH,** Laporte SA, Holt JA, Barak LS, Caron MG (2001) Molecular Determinants Underlying the Formation of Stable Intracellular G Protein-coupled Receptor-β-Arrestin Complexes after Receptor Endocytosis*. *Journal of Biological Chemistry* **276**:19452-19460 https://doi.org/10.1074/jbc.M101450200

**Oakley RH,** Laporte SA, Holt JA, Caron MG, Barak LS (2000) Differential Affinities of Visual Arrestin, βArrestin1, and βArrestin2 for G Protein-coupled Receptors Delineate Two Major Classes of Receptors*. *Journal of Biological Chemistry* **275**:17201-17210 https://doi.org/10.1074/jbc.M910348199

**Otero C,** Groettrup M, Legler DF (2006) Opposite Fate of Endocytosed CCR7 and Its Ligands: Recycling versus Degradation1. *The Journal of Immunology* **177**:2314-2323 https://doi.org/10.4049/jimmunol.177.4.2314

**Patterson BK,** Seethamraju H, Dhody K, Corley MJ, Kazempour K, Lalezari J, Pang APS, Sugai C, Mahyari E, Francisco EB, *et al.* (2021) CCR5 inhibition in critical COVID-19 patients decreases inflammatory cytokines, increases CD8 T-cells, and decreases SARS-CoV2 RNA in plasma by day 14. *International Journal of Infectious Diseases* **103**:25-32 https://doi.org/10.1016/j.ijid.2020.10.101

**Popova NV,** Deyev IE, Petrenko AG (2013) Clathrin-Mediated Endocytosis and Adaptor Proteins. *Acta Naturae* **5**:62-73

**Schindelin J,** Arganda-Carreras I, Frise E, Kaynig V, Longair M, Pietzsch T, Preibisch S, Rueden C, Saalfeld S, Schmid B, *et al.* (2012) Fiji: an open-source platform for biological-image analysis. *Nat Methods* **9**:676-682 https://doi.org/10.1038/nmeth.2019

**Schmid EM,** Ford MGJ, Burtey A, Praefcke GJK, Peak-Chew S-Y, Mills IG, Benmerah A, McMahon HT (2006) Role of the AP2 β-Appendage Hub in Recruiting Partners for Clathrin-Coated Vesicle Assembly. *PLOS Biology* **4**:e262 https://doi.org/10.1371/journal.pbio.0040262

**Schneider CA,** Rasband WS, Eliceiri KW (2012) NIH Image to ImageJ: 25 years of image analysis. *Nat Methods* **9**:671-675 https://doi.org/10.1038/nmeth.2089

**Shiraishi Y,** Kofuku Y, Ueda T, Pandey S, Dwivedi-Agnihotri H, Shukla AK, Shimada I (2021) Biphasic activation of β-arrestin 1 upon interaction with a GPCR revealed by methyl-TROSY NMR. *Nat Commun* **12**:7158 https://doi.org/10.1038/s41467-021-27482-3

**Signoret N,** Hewlett L, Wavre S, Pelchen-Matthews A, Oppermann M, Marsh M (2005) Agonist-induced Endocytosis of CC Chemokine Receptor 5 Is Clathrin Dependent. *Mol Biol Cell* **16**:902-917 https://doi.org/10.1091/mbc.E04-08-0687

**Skinner SP,** Fogh RH, Boucher W, Ragan TJ, Mureddu LG, Vuister GW (2016) CcpNmr AnalysisAssign: a flexible platform for integrated NMR analysis. *J Biomol NMR* **66**:111-124 https://doi.org/10.1007/s10858-016-0060-y

**Smith CJ,** Grigorieff N, Pearse BMF (1998) Clathrin coats at 21 Å resolution: a cellular assembly designed to recycle multiple membrane receptors. *The EMBO Journal* **17**:4943-4953 https://doi.org/10.1093/emboj/17.17.4943

**Smith SM,** Baker M, Halebian M, Smith CJ (2017) Weak Molecular Interactions in Clathrin-Mediated Endocytosis. *Frontiers in Molecular Biosciences* **4**

**Smith SM,** Smith CJ (2022) Capturing the mechanics of clathrin-mediated endocytosis. *Current Opinion in Structural Biology* **75**:102427 https://doi.org/10.1016/j.sbi.2022.102427

**Tohgo A,** Choy EW, Gesty-Palmer D, Pierce KL, Laporte S, Oakley RH, Caron MG, Lefkowitz RJ, Luttrell LM (2003) The Stability of the G Protein-coupled Receptor-β-Arrestin Interaction Determines the Mechanism and Functional Consequence of ERK Activation *. *Journal of Biological Chemistry* **278**:6258-6267 https://doi.org/10.1074/jbc.M212231200

**Tugarinov V,** Hwang PM, Ollerenshaw JE, Kay LE (2003) Cross-Correlated Relaxation Enhanced 1H−13C NMR Spectroscopy of Methyl Groups in Very High Molecular Weight Proteins and Protein Complexes. *J Am Chem Soc* **125**:10420-10428 https://doi.org/10.1021/ja030153x

**Tugarinov V,** Kanelis V, Kay LE (2006) Isotope labeling strategies for the study of high-molecular-weight proteins by solution NMR spectroscopy. *Nat Protoc* **1**:749-754 https://doi.org/10.1038/nprot.2006.101

**Violin JD,** Ren X-R, Lefkowitz RJ (2006) G-protein-coupled receptor kinase specificity for beta-arrestin recruitment to the beta2-adrenergic receptor revealed by fluorescence resonance energy transfer. *J Biol Chem* **281**:20577-20588 https://doi.org/10.1074/jbc.M513605200

**Weis WI,** Kobilka BK (2018) The Molecular Basis of G Protein–Coupled Receptor Activation. *Annual Review of Biochemistry* **87**:897-919 https://doi.org/10.1146/annurev-biochem-060614-033910

**Wiktor M,** Hartley O, Grzesiek S (2013) Characterization of Structure, Dynamics, and Detergent Interactions of the Anti-HIV Chemokine Variant 5P12-RANTES. *Biophysical Journal* **105**:2586-2597 https://doi.org/10.1016/j.bpj.2013.10.025

**Wolfe BL,** Trejo J (2007) Clathrin-Dependent Mechanisms of G Protein-coupled Receptor Endocytosis. *Traffic* **8**:462-470 https://doi.org/10.1111/j.1600-0854.2007.00551.x

**Xiao K,** Shenoy SK, Nobles K, Lefkowitz RJ (2004) Activation-dependent Conformational Changes in β-Arrestin 2*. *Journal of Biological Chemistry* **279**:55744-55753 https://doi.org/10.1074/jbc.M409785200

**Zeng Z,** Lan T, Wei Y, Wei X (2022) CCL5/CCR5 axis in human diseases and related treatments. *Genes & Diseases* **9**:12-27 https://doi.org/10.1016/j.gendis.2021.08.004

**Zhuo Y,** Cano KE, Wang L, Ilangovan U, Hinck AP, Sousa R, Lafer EM (2015) Nuclear Magnetic Resonance Structural Mapping Reveals Promiscuous Interactions between Clathrin-Box Motif Sequences and the N-Terminal Domain of the Clathrin Heavy Chain. *Biochemistry* **54**:2571-2580 https://doi.org/10.1021/acs.biochem.5b00065

# Peer reviews

## Reviewer #1 (Public review):

Petrovic et al. investigate CCR5 endocytosis via arrestin2, with a particular focus on clathrin and AP2 contributions. The study is thorough and methodologically diverse. The NMR titration data clearly demonstrate chemical shift changes at the canonical clathrin-binding site (LIELD), present in both the 2S and 2L arrestin splice variants. To assess the effect of arrestin activation on clathrin binding, the authors compare: truncated arrestin (1-393), full-length arrestin, and 1-393 incubated with CCR5 phosphopeptides. All three bind clathrin comparably, whereas controls show no binding. These findings are consistent with prior crystal structures showing peptide-like binding of the LIELD motif, with disordered flanking regions. The manuscript also evaluates a non-canonical clathrin binding site specific to the 2L splice variant. Though this region has been shown to enhance beta2-adrenergic receptor binding, it appears not to affect CCR5 internalization.

Similar analyses applied to AP2 show a different result. AP2 binding is activation-dependent and influenced by the presence and level of phosphorylation of CCR5-derived phosphopeptides. These findings are reinforced by cellular internalization assays.

In sum, the results highlight splice-variant-dependent effects and phosphorylation-sensitive arrestin-partner interactions. The data argue against a (rapidly disappearing) one-size-fits-all model for GPCR-arrestin signaling and instead support a nuanced, receptor-specific view, with one example summarized effectively in the mechanistic figure.

https://doi.org/10.7554/eLife.106839.3.sa3

## Reviewer #2 (Public review):

Summary:

Based on extensive live cell assays, SEC, and NMR studies of reconstituted complexes, these authors explore the roles of clathrin and the AP2 protein in facilitating clathrin mediated endocytosis via activated arrestin-2. NMR, SEC, proteolysis, and live cell tracking confirm a strong interaction between AP2 and activated arrestin using a phosphorylated C-terminus of CCR5. At the same time a weak interaction between clathrin and arrestin-2 is observed, irrespective of activation.

These results contrast with previous observations of class A GPCRs and the more direct participation by clathrin. The results are discussed in terms of the importance of short and

long phosphorylated bar codes in class A and class B endocytosis.

Strengths:

The 15N,1H and 13C,methyl TROSY NMR and assignments represent a monumental amount of work on arrestin-2, clathrin, and AP2. Weak NMR interactions between arrestin-2 and clathrin are observed irrespective of activation of arrestin. A second interface, proposed by crystallography, was suggested to be a possible crystal artifact. NMR establishes realistic information on the clathrin and AP2 affinities to activated arrestin with both kD and description of the interfaces.

https://doi.org/10.7554/eLife.106839.3.sa2

## Reviewer #3 (Public review):

Summary:

Overall, this is a well-done study, and the conclusions are largely supported by the data, which will be of interest to the field.

Strengths:

Strengths of this study include experiments with solution NMR that can resolve high-resolution interactions of the highly flexible C-terminal tail of arr2 with clathrin and AP2. Although mainly confirmatory in defining the arr2 CBL 376LIELD380 as the clathrin binding site, the use of the NMR is of high interest (Fig. 1). The 15N-labeled CLTC-NTD experiment with arr2 titrations reveals a span from 39-108 that mediates an arr2 interaction, which corroborates previous crystal data, but does not reveal a second area in CLTC-NTD that in previous crystal structures was observed to interact with arr2.

SEC and NMR data suggest that full-length arr2 (1-418) binding with 2-adaptin subunit of AP2 is enhanced in the presence of CCR5 phospho-peptides (Fig. 3). The pp6 peptide shows the highest degree of arr2 activation, and 2-adaptin binding, compared to less phosphorylated peptide or not phosphorylated at all. It is interesting that the arr2 interaction with CLTC NTD and pp6 cannot be detected using the SEC approach, further suggesting that clathrin binding is not dependent on arrestin activation. Overall, the data suggest that receptor activation promotes arrestin binding to AP2, not clathrin, suggesting the AP2 interaction is necessary for CCR5 endocytosis.

To validate the solid biophysical data, the authors pursue validation experiments in a HeLa cell model by confocal microscopy. This requires transient transfection of tagged receptor (CCR5-Flag) and arr2 (arr2-YFP). CCR5 displays a "class B"-like behavior in that arr2 is rapidly recruited to the receptor at the plasma membrane upon agonist activation, which forms a stable complex that internalizes onto endosomes (Fig. 4). The data suggest that complex internalization is dependent on AP2 binding not clathrin (Fig. 5).

The addition of the antagonist experiment/data adds rigor to the study.

Overall, this is a solid study that will be of interest to the field.

https://doi.org/10.7554/eLife.106839.3.sa1

## Author response:

The following is the authors' response to the previous reviews

> ***eLife Assessment***

> *The authors investigate arrestin2-mediated CCR5 endocytosis in the context of clathrin and AP2 contributions. Using an extensive set of NMR experiments, and supported by microscopy and other biophysical assays, the authors provide compelling data on the roles of AP2 and clathrin in CCR5 endocytosis. This important work will appeal to an audience beyond those studying chemokine receptors, including those studying GPCR regulation and trafficking. The distinct role of AP2 and not clathrin will be of particular interest to those studying GPCR internalization mechanisms.*
>
> ***Public Reviews:***
>
> ***Reviewer #1 (Public review):***
>
> *Petrovic et al. investigate CCR5 endocytosis via arrestin 2, with a particular focus on clathrin and AP2 contributions. The study is thorough and methodologically diverse. The NMR titration data clearly demonstrate chemical shift changes at the canonical clathrin-binding site (LIELD), present in both the 2S and 2L arrestin splice variants.*
>
> *To assess the effect of arrestin activation on clathrin binding, the authors compare: truncated arrestin (1-393), full-length arrestin, and 1-393 incubated with CCR5 phosphopeptides. All three bind clathrin comparably, whereas controls show no binding. These findings are consistent with prior crystal structures showing peptide-like binding of the LIELD motif, with disordered flanking regions. The manuscript also evaluates a non-canonical clathrin binding site specific to the 2L splice variant. Though this region has been shown to enhance beta2-adrenergic receptor binding, it appears not to affect CCR5 internalization.*
>
> *Similar analyses applied to AP2 show a different result. AP2 binding is activation-dependent and influenced by the presence and level of phosphorylation of CCR5-derived phosphopeptides. These findings are reinforced by cellular internalization assays.*
>
> *In sum, the results highlight splice-variant-dependent effects and phosphorylation-sensitive arrestin-partner interactions. The data argue against a (rapidly disappearing) one-size-fitsall model for GPCR-arrestin signaling and instead support a nuanced, receptor-specific view, with one example summarized effectively in the mechanistic figure.*

We thank the referee for this positive assessment of our manuscript. Indeed, by stepping away from the common receptor models for understanding internalization (b2AR and V2R), we revealed the phosphorylation level of the receptor as a key factor in driving the sequestration of the receptor from the plasma membrane. We hope that the proposed mechanistic model will aid further studies to obtain an even more detailed understanding of forces driving receptor internalization.

> *Weaknesses:*
>
> *Figure 1 shows regions alphaFold model that are intrinsically disordered without making it clear that this is not an expected stable position. The authors NMR titration data are n=1. Many figure panels require that readers pinch and zoom to see the data.*

In the “Recommendations for the Authors” section, we addressed the reviewer’s stated weaknesses. In short, for the AlphaFold representation in Figure 1A, we added explicit labeling and revised the legend and main text to clearly state that the depicted loops are intrinsically disordered, absent from crystal structures due to flexibility, and shown only for visualization of their location. We also clarified that the NMR titration experiments inherently have n = 1 due to technical limitations, and that this is standard practice in the field, while ensuring individual data points remain visible. The supplementary NMR figures

now have more vibrant coloring, allowing easier data assessment. However, we have not changed the zooming of the microscopy and NMR spectra. We believe that the presentation of microscopy data, which already show zoomed-in regions of interest, follow standard practices in the field. Furthermore, we strongly believe that we should display full NMR spectra in the supplementary figures to allow the reader to assess the overall quality and behavior. As indicated previously, the reader can zoom in to very high resolution, since the spectra are provided by vector graphics. Zoomed regions of the relevant details are provided in the main figures.

> ***Reviewer #2 (Public review):***
>
> *Summary:*
>
> *Based on extensive live cell assays, SEC, and NMR studies of reconstituted complexes, these authors explore the roles of clathrin and the AP2 protein in facilitating clathrin mediated endocytosis via activated arrestin-2. NMR, SEC, proteolysis, and live cell tracking confirm a strong interaction between AP2 and activated arrestin using a phosphorylated C-terminus of CCR5. At the same time a weak interaction between clathrin and arrestin-2 is observed, irrespective of activation.*
>
> *These results contrast with previous observations of class A GPCRs and the more direct participation by clathrin. The results are discussed in terms of the importance of short and long phosphorylated bar codes in class A and class B endocytosis.*
>
> *Strengths:*
>
> *The 15N,1H and 13C,methyl TROSY NMR and assignments represent a monumental amount of work on arrestin-2, clathrin, and AP2. Weak NMR interactions between arrestin-2 and clathrin are observed irrespective of activation of arrestin. A second interface, proposed by crystallography, was suggested to be a possible crystal artifact. NMR establishes realistic information on the clathrin and AP2 affinities to activated arrestin with both kD and description of the interfaces.*

We sincerely thank the referee for this encouraging evaluation of our work and appreciate the recognition of the NMR efforts and insights into the arrestin–clathrin–AP2 interactions.

> *Weaknesses:*
>
> *This reviewer has identified only minor weaknesses with the study.*
>
> *(1) I don't observe two overlapping spectra of Arrestin2 (1393) +/- CLTC NTD in Supp Figure 1*

We believe the referee is referring to Figure 1 – figure supplement 2. We have now made the colors of the spectra more vibrant and used different contouring to make the differences between the two spectra clearer. The spectra are provided as vector graphics, which allows zooming in to the very fine details.

> *(2) Arrestin-2 1-418 resonances all but disappear with CCR5pp6 addition. Are they recovered with Ap2Beta2 addition and is this what is shown in Supp Fig 2D*

We believe the reviewer is referring to Figure 3 - figure supplement 1. In this figure, the panels E and F show resonances of arrestin2$^{1\text{-}418}$ (apo state shown with black outline) disappear upon the addition of CCR5pp6 (arrestin2$^{1\text{-}418}$•CCR5pp6 complex spectrum in red). The panels C and D show resonances of arrestin2$^{1\text{-}418}$ (apo state shown with black outline), which remain unchanged upon addition of AP2b2 $^{701\text{-}937}$ (orange), indicating no complex formation. We also recorded a spectrum of the arrestin2$^{1\text{-}418}$•CCR5pp6 complex under addition of AP2b2 $^{701\text{-}937}$ (not shown), but the arrestin2 resonances in the arrestin2$^{1\text{-}418}$

•CCR5pp6 complex were already too broad for further analysis. This had been already explained in the text.

“In agreement with the AP2b2 NMR observations, no interaction was observed in the arrestin2 methyl and backbone NMR spectra upon addition of AP2b2 in the absence of phosphopeptide (Figure 3-figure supplement 1C, D). However, the significant line broadening of the arrestin2 resonances upon phosphopeptide addition (Figure 3-figure supplement 1E, F) precluded a meaningful assessment of the effect of the AP2b2 addition on arrestin2 in the presence of phosphopeptide”.

> *(3) I don't understand how methyl TROSY spectra of arrestin2 with phosphopeptide could look so broadened unless there are sample stability problems?*

We thank the referee for this comment. We would like to clarify that in general a broadened spectrum beyond what is expected from the rotational correlation time does not necessarily correlate with sample stability problems. It is rather evidence of conformational intermediate exchange on the micro- to millisecond time scale.

The displayed $^{1}$H-$^{15}$N spectra of apo arrestin2 already suffer from line broadening due to such intrinsic mobility of the protein. These spectra were recorded with acquisition times of 50 ms ($^{15}$N) and 55 ms ($^{1}$H) and resolution-enhanced by a 60°shifted sine-bell filter for $^{15}$N and a 60°shifted squared sine-bell filter for $^{1}$H, respectively, which leads to the observed resolution with still reasonable sensitivity. The $^{1}$H-$^{15}$N resonances in Fig. 1b (arrestin2$^{1\text{-}393}$) look particularly narrow. However, this region contains a large number of flexible residues. The full spectrum, e.g. Figure 1-figure supplement 2, shows the entire situation with a clear variation of linewidths and intensities. The linewidth variation becomes stronger when omitting the resolution enhancement filters.

The addition of the CCR5pp6 phosphopeptide does not change protein stability, which we assessed by measuring the melting temperature of arrestin2$^{1\text{-}418}$ and arrestin2$^{1\text{-}418}$•CCR5pp6 complex (Tm = 57°C in both cases). We believe that the explanation for the increased broadening of the arrestin2 resonances is that addition of the CCR5pp6, possibly due to the release of the arrestin2 strand b20, amplifies the mentioned intermediate timescale protein dynamics. This results in the disappearance of arrestin2 resonances.

We have now included the assessment of arrestin2$^{1\text{-}418}$ and arrestin2$^{1\text{-}418}$•CCR5pp6 stability in the manuscript:

“The observed line broadening of arrestin2 in the presence of phosphopeptide must be a result of increased protein motions and is not caused by a decrease in protein stability, since the melting temperature of arrestin2 in the absence and presence of phosphopeptide are identical (56.9 ± 0.1 °C)”.

> *(4) At one point the authors added excess fully phosphorylated CCR5 phosphopeptide (CCR5pp6). Does the phosphopeptide rescue resolution of arrestin2 (NH or methyl) to the point where interaction dynamics with clathrin (CLTC NTD) are now more evident on the arrestin2 surface?*

Unfortunately, when we titrate arrestin2 with CCR5pp6 (please see Isaikina & Petrovic et. al, Mol. Cell, 2023 for more details), the arrestin2 resonances undergo fast-to-intermediate exchange upon binding. In the presence of phosphopeptide excess, very few resonances remain, the majority of which are in the disordered region, including resonances from the clathrin-binding loop. Due to the peak overlap, we could not unambiguously assign arrestin2 resonances in the bound state, which precluded our assessment of the arrestin2-clathrin interaction in the presence of phosphopeptide. We have made this now clearer in the paragraph ‘The arrestin2-clathrin interaction is independent of arrestin2 activation’

"Due to significant line broadening and peak overlap of the arrestin2 resonances upon phosphopeptide addition, the influence of arrestin activation on the clathrin interaction could not be detected on either backbone or methyl resonances ".

> *(5) Once phosphopeptide activates arrestin-2 and AP2 binds can phosphopeptide be exchanged off? In this case, would it be possible for the activated arrestin-2 AP2 complex to re-engage a new (phosphorylated) receptor?*

This would be an interesting mechanism. In principle, this should be possible as long as the other (phosphorylated) receptor outcompetes the initial phosphopeptide with higher affinity towards the binding site. However, we do not have experiments to assess this process directly. Therefore, we rather wish not to further speculate.

> *(6) I'd be tempted to move the discussion of class A and class B GPCRs and their presumed differences to the intro and then motivate the paper with specific questions.*

We appreciate the referee's suggestion and had a similar idea previously. However, as we do not have data on other class-A or class-B receptors, we rather don't want to motivate the entire manuscript by this question.

> *(7) Did the authors ever try SEC measurements of arrestin-2 + AP2beta2+CCR5pp6 with and without PIP2, and with and without clathrin (CLTC NTD? The question becomes what the active complex is and how PIP2 modulates this cascade of complexation events in class B receptors.*

We thank the referee for this question. Indeed, we tested whether PIP2 can stabilize the arrestin2•CCR5pp6•AP2 complex by SEC experiments. Unfortunately, the addition of PIP2 increased the formation of arrestin2 dimers and higher oligomers, presumably due to the presence of additional charges. The resolution of SEC experiments was not sufficient to distinguish arrestin2 in oligomeric form or in arrestin2•CCR5pp6•AP2 complex. We now mention this in the text:

"We also attempted to stabilize the arrestin2-AP2b2-phosphopetide complex through the addition of PIP2, which can stabilize arrestin complexes with the receptor (Janetzko et al., 2022). The addition of PIP2 increased the formation of arrestin2 dimers and higher oligomers, presumably due to the presence of additional charges. Unfortunately, the resolution of the SEC experiments was not sufficient to separate the arrestin2 oligomers from complexes with AP2b2".

> ***Reviewer #3 (Public review):***
>
> *Summary:*
>
> *Overall, this is a well-done study, and the conclusions are largely supported by the data, which will be of interest to the field.*
>
> *Strengths:*
>
> *Strengths of this study include experiments with solution NMR that can resolve high-resolution interactions of the highly flexible C-terminal tail of arr2 with clathrin and AP2. Although mainly confirmatory in defining the arr2 CBL376LIELD380 as the clathrin binding site, the use of the NMR is of high interest (Fig. 1). The 15N-labeled CLTC-NTD experiment with arr2 titrations reveals a span from 39-108 that mediates an arr2 interaction, which corroborates previous crystal data, but does not reveal a second area in CLTC-NTD that in previous crystal structures was observed to interact with arr2.*

> *SEC and NMR data suggest that full-length arr2 (1-418) binding with 2-adaptin subunit of AP2 is enhanced in the presence of CCR5 phospho-peptides (Fig. 3). The pp6 peptide shows the highest degree of arr2 activation, and 2-adaptin binding, compared to less phosphorylated peptide or not phosphorylated at all. It is interesting that the arr2 interaction with CLTC NTD and pp6 cannot be detected using the SEC approach, further suggesting that clathrin binding is not dependent on arrestin activation. Overall, the data suggest that receptor activation promotes arrestin binding to AP2, not clathrin, suggesting the*
>
> *AP2 interaction is necessary for CCR5 endocytosis.*
>
> *To validate the solid biophysical data, the authors pursue validation experiments in a HeLa cell model by confocal microscopy. This requires transient transfection of tagged receptor (CCR5-Flag) and arr2 (arr2-YFP). CCR5 displays a "class B"-like behavior in that arr2 is rapidly recruited to the receptor at the plasma membrane upon agonist activation, which forms a stable complex that internalizes onto endosomes (Fig. 4). The data suggest that complex internalization is dependent on AP2 binding not clathrin (Fig. 5).*
>
> *The addition of the antagonist experiment/data adds rigor to the study.*
>
> *Overall, this is a solid study that will be of interest to the field.*

We thank the referee for the careful and encouraging evaluation of our work. We appreciate the recognition of the solidity of our data and the support for our conclusions regarding the distinct roles of AP2 and clathrin in arrestin-mediated receptor internalization.

> ***Recommendations for the authors:***
>
> ***Reviewer #1 (Recommendations for the authors):***
>
> *I believe that the authors have made efforts to improve the accessibility to a broader audience. In a few cases, I believe that the authors response either did not truly address the concern or made the problem worse. I am grouping these as 'very strong opinions' and 'sticking point'.*
>
> *Very strong opinion 1:*
>
> *While data presentation is somewhat at the authors discretion, there were several figures where the presentation did not make the work approachable, including microscopy insets and NMR spectra. A suggestion to 'pinch and zoom' does not really address this. For the overlapping NMR spectra in supporting Figure 1, I actually -can- see this on zooming, but I did not recognize this on first pass because the colors are almost identical for the two spectra. This is an easy fix. Changing the presentation by coloring these distinctly would alleviate this. The Supplemental figure to Fig. 2 looks strange with pinch and zoom. But at the end of the day, data presentation where the reader is to infer that they must zoom in is not very approachable and may prevent readers from being able to independently assess the data. In this case, there doesn't seem to be a strong rationale to not make these panels easier to see at 100% size.*

We appreciate the reviewer's thoughtful comments regarding figure accessibility and agree that data presentation should be clear and interpretable without requiring readers to zoom in extensively. However, we must note that the presentation of the microscopy data follows standard practices in the field and that the panels already include zoomed-in regions, which enable easier access to key results and observations.

Regarding the NMR data, we have revised Figure 1—figure supplement 2 and Figure 2—figure supplement 1 to match the presentation style of Figure 3—figure supplement 1, which the reviewer apparently found more accessible. We also made the colors of the spectra more vibrant, as the referee suggested. We would like to emphasize that it is absolutely necessary to display the full NMR spectra in order to allow independent assessment of signal assignment, data quality, and overall protein behavior. Zoomed regions of the relevant details are provided in the main figures.

> *Very strong opinion 2:*
>
> *The author's response to lack of individual data points and error bars is that this is an n=1 experiment. I do not believe this meets the minimum standard for best practices in the field.*

We respectfully disagree with the reviewer's assessment. The Figure already displays individual data points, as shown already in the initial submission. Performing NMR titrations with isotopically labeled protein samples is inherently resource-intensive, and single-sample (n = 1) experiments are widely accepted and routinely reported in the field. Numerous studies have used the same approach, including Rosenzweig et al., Science (2013); Nikolaev et al., Nat. Methods (2019); and Hobbs et al., J. Biomol. NMR (2022), as well as our own recent work (Isaikina & Petrovic et al., Mol. Cell, 2023). These studies demonstrate that such NMR-based affinity measurements, even when performed on a single sample, are highly reproducible, precise, and consistent with orthogonal evidence and across different sample conditions.

> *Sticking point:*
>
> *Figure 1A - the alphaFold model of arrestin2L depicts the disordered loops as ordered. The depiction is misleading at best, and inaccurate in truth. To use an analogy, what the authors depict is equivalent to publishing an LLM hallucination in the text. Unlike LLMs, alphaFold will actually flag its hallucination with the confidence (pLDDT) in the output. Both for LLMs and for alphaFold, we are spending much time teaching our students in class how to use computation appropriately - both to improve efficiency but also to ensure accuracy by removing hallucinations.*
>
> *The original review indicated that confidences needed to be shown and that this needed to be depicted in a way that clarifies that this is NOT a structural state of the loops. The newly added description ("The model was used to visualize the clathrin-binding loop and the 344-loop of the arrestin2 Cdomain, which are not detected in the available crystal structures...) worsens the concern because it even more strongly implies that a 0 confidence computational output is a likely structural state. It also indicates that these regions were 'not detected' in crystal structures. These regions of arrestin are intrinsically disordered. AlphaFold (by it's nature) must put out something in terms of coordinates, even if the pLDDT suggests that the region cannot be predicted or is not in a stable position, which is the case here. In crystal structures, these regions are not associated with interpretable electron density, meaning that coordinates are omitted in these regions because adding them would imply that under the conditions used, the protein adopts a low energy structural state in this region. This region is instead intrinsically disordered.*
>
> *A good description of why showing disordered loops in a defined position is incorrect and how to instead depict disorder correctly is in Brotzakis et al. Nat communications 16, 1632 (2025) "AlphaFold prediction of structural ensembles of disordered proteins", where figures 3A, 4A, and 5A show one AlphaFold prediction colored by confidence and 3B, 4B and 5B are more accurate depictions of the structural ensemble.*

> *Coming back to the original comment "The AlphaFold model could benefit from a more transparent discussion of prediction confidence and caveats. The younger crowd (part of the presumed intended readership) tends to be more certain that computational output is 'true'...." Right now, the authors are still showing in Fig 1A a depiction of arrestin with models for the loops that are untrue. They now added text indicating that these loops are visualized in an AlphaFold prediction and 'true' but 'not detected in crystal structures'. There is no indication in the text that these are intrinsically disordered. The lack of showing the pLDDT confidence and the lack of any indication that these are disordered regions is simply incorrect.*

We appreciate the concern of the reviewer towards AlphaFold models. As NMR spectroscopists we are highly aware of intrinsic biomolecular motions. However, our AlphaFold2 model is used as a graphical representation to display the interaction sites of loops; it is not intended to depict the loops as fixed structural states. The flexibility of the loops had been clearly described in the main text before:

“Arrestin2 consists of two consecutive (N- and C-terminal) β-sandwich domains (Figure 1A), followed by the disordered clathrin-binding loop (CBL, residues 353–386), strand b20 (residues 386–390), and a disordered C-terminal tail after residue 393”.

and

“Figure 1B depicts part of a 1H-15N TROSY spectrum (full spectrum in Figure 1-figure supplement 2A) of the truncated 15N-labeled arrestin2 construct arrestin21-393 (residues 1393), which encompasses the C-terminal strand β20, but lacks the disordered C-terminal tail. Due to intrinsic microsecond dynamics, the assignment of the arrestin21-393 1H-15N resonances by triple resonance methods is largely incomplete, but 16 residues (residues 367381, 385-386) within the mobile CBL could be assigned. This region of arrestin is typically not visible in either crystal or cryo-EM structures due to its high flexibility”.

as well as in the legend to Figure 1:

“The model was used to visualize the clathrin-binding loop and the 344-loop of the arrestin2 C-domain, which are not detected in the available crystal structures of apo arrestin2 [bovine: PDB 1G4M (Han et al., 2001), human: PDB 8AS4 (Isaikina et al., 2023)]. In the other structured regions, the model is virtually identical to the crystal structures”.

We have now further added a label ‘AlphaFold2 model’ to Figure 1A and amended the respective Figure legend to

“The model was used to visualize the clathrin-binding loop and the 344-loop of the arrestin2 C-domain, which are not detected in the available crystal structures of apo arrestin2 [bovine: PDB 1G4M (Han et al., 2001), human: PDB 8AS4 (Isaikina et al., 2023)] due to flexibility. In the other structured regions, the model is virtually identical to the crystal structures”.

> ***Reviewer #2 (Recommendations for the authors):***
>
> *I appreciated the response by the authors to all of my questions. I have no further comments*

We thank the referee for the raised questions, which we believe have improved the quality of the manuscript.

https://doi.org/10.7554/eLife.106839.3.sa0